

Gravitational instability via the Schrödinger equation

C J Short and P Coles

School of Physics and Astronomy, University of Nottingham, University Park,
Nottingham, UK, NG7 2RD

E-mail: ppxcjs@nottingham.ac.uk, peter.coles@nottingham.ac.uk

Abstract. We study an approach to the formation of large-scale structure in the universe based on the description of a self-gravitating fluid in terms of a Schrödinger equation coupled to the usual Poisson equation. This approach has a number of promising features, but also some peculiarities. In this exploratory paper we discuss the behaviour of perturbations of the Schrödinger-Poisson system in simple one-dimensional configurations and compare the results with more conventional approaches: linear perturbation theory of the fluid equations and the Zeldovich approximation. The results demonstrate that our approach furnishes a useful addition to the repertoire of analytical techniques available for the description of cosmological perturbations, but that there are a number of subtleties to be faced when this method is applied in practice. In particular, care must be taken in choosing appropriate values for the effective Planck constant in the theory.

PACS numbers: 95.35.+d, 98.65.Dx, 98.80.-k

Submitted to: *J. Cosmol. Astropart. Phys.*

1. Introduction

The local universe displays a rich hierarchical pattern of galaxy clustering that encompasses a vast range of length scales, culminating in rich clusters and super-clusters. However, the early universe was almost smooth, with only slight ripples seen in the cosmic microwave background radiation. Models of the formation of structure link these observations through the effect of gravity, relying on the fact that small initially over-dense regions accrete additional matter as the universe expands. During the early stages the ripples evolve independently, like linear waves on the surface of deep water. As the structures grow in mass, the modes couple together in a non-linear fashion, more like the behaviour of waves breaking in shallow water.

The linear theory of perturbation growth resulting from gravitational instability is well-established, but the non-linear regime is much more complicated and generally not amenable to analytic solution. Numerical N -body simulations have led the way

towards an understanding of strongly developed clustering. Although such calculations have been priceless in establishing quantitative predictions of the large-scale structure expected to arise in particular cosmogonies, it remains important to develop as full an analytical understanding as possible. After all, simulating a thing is not quite equivalent to understanding it.

Analytical techniques for handling the evolution of cosmological density perturbations into the non-linear regime fall into two broad classes. First there are techniques based on applying perturbation theory to a fluid description of the self-gravitating matter. These Eulerian approaches range from simple first-order (linear) perturbation theory for the evolution of the density field (e.g. Peebles 1980) through to higher-order approaches of vastly increased complexity (e.g. Bernardeau et al. 2002). Alternatively one can begin with a description of the trajectories of matter particles and perturb these rather than the macroscopic fluid quantities. Even the simplest of these (Lagrangian) approaches, the Zeldovich approximation (Zeldovich 1970), has proved highly successful in comparison against full N -body calculations in describing the quantitative morphology of the clustering pattern (Coles *et al* 1993). For a review of both these approaches, see Sahni and Coles (1995).

The Eulerian and Lagrangian approaches have strengths and weaknesses. Linear perturbation theory (LPT) of cosmological fluids has been the mainstay of structure formation theory for many decades, by virtue of its simplicity and its robustness on large scales where the density fluctuations are known to be very much smaller than the mean density. When extrapolated to smaller scales, it provides a useful indicative measure of clustering strength, but does generate some absurdities if taken too far. Such perturbative techniques, for example, impose no requirement that the overall matter density field should be positive definite. Lagrangian approaches do not suffer from this particular problem, but they display an alternative kind of pathology. When particle trajectories cross (a phenomenon known as *shell-crossing*), the derived density field develops a singularity and the approach fails.

In this paper we study an alternative and radically different approach that combines attractive features of both Eulerian and Lagrangian approaches. Based on an original suggestion by Widrow and Kaiser (1993), we describe the cosmological density field not as a classical fluid, but in terms of the Schrödinger equation of quantum mechanics; see Widrow (1997) for a relativistic extension of the original Newtonian theory. The reasoning behind this is not new - in essence it dates back to Madelung (1926) - but it is quite neglected in the cosmological setting. Coles (2002) showed that this approach provides a natural explanation of why the distribution function of density fluctuations, evolved from Gaussian initial conditions, should be close to the log-normal form that is observed. This, and other attractive properties of perturbations in the wave-mechanical description were discussed by Szapudi and Kaiser (2003). Coles and Spencer (2003) demonstrated how this approach fares in comparison with the Zeldovich approximation for particular examples of self-gravitating collapse; we will build on this work in this paper.

Our goal in this work is to explore the basic perturbative properties of this novel approach to structure formation in cosmology. We do this by considering simple idealized examples of one-dimensional gravitational collapse. Clearly the results we obtain are not in a form that can be directly compared with observations or full numerical calculations of structure formation. Instead our intention is to elucidate some of the subtleties that must be faced when applying this (admittedly rather strange) method in practice. We defer the more practical aspects of this study (including a full systematic comparison with numerical simulations) to a subsequent paper (Short and Coles 2006).

The outline of this paper is as follows. First, in order to keep the paper as self-contained and pedagogically informative as possible we briefly outline the basic theory of cosmological structure formation, including the standard fluid perturbation theory, the Zeldovich approximation and the wave-mechanical approach. Next, in section 3 we apply the wave-mechanical approximation to simple one-dimensional collapse scenarios. We describe how to construct perturbative solutions to the Schrödinger equation in each example we consider. In section 4 we present our results and discuss the general properties of our wave-mechanical approach in detail. We conclude in section 5.

2. Cosmological structure formation

The Big Bang model is built upon the Cosmological Principle, a symmetry principle that requires the universe on large scales to be both homogeneous and isotropic. Space-times consistent with this requirement are described by the Robertson–Walker metric

$$ds^2 = c^2 dt^2 - a^2 \left(\frac{dr^2}{1 - \kappa r^2} + r^2 d\theta^2 + r^2 \sin^2 \theta d\phi^2 \right), \quad (1)$$

where c is the speed of light and κ is the spatial curvature, scaled so as to take the values 0 or ± 1 . The case $\kappa = 0$ represents flat space sections, and the other two cases correspond to space sections of constant positive or negative curvature, respectively. The time coordinate t is *cosmological proper time* and it is singled out as a preferred time coordinate by the property of spatial homogeneity. The quantity $a = a(t)$ is the *cosmological scale factor*, describing the overall expansion of the universe as a function of proper time. The spatial coordinates (r, θ, ϕ) are comoving spherical polar coordinates.

The dynamics of a universe described by the metric (1) are governed by the Friedmann equations:

$$H^2 = \frac{8\pi G}{3} \rho_b - \frac{\kappa c^2}{a^2} + \frac{\Lambda}{3}, \quad (2)$$

$$\frac{\ddot{a}}{a} = -\frac{4\pi G}{3} \left(\rho_b + \frac{3P_b}{c^2} \right) + \frac{\Lambda}{3}, \quad (3)$$

$$\dot{\rho}_b = -3H \left(\rho_b + \frac{P_b}{c^2} \right), \quad (4)$$

where Λ is the *cosmological constant* and $H = H(t)$ is the Hubble parameter, defined by $H \equiv \dot{a}/a$. Dots are used throughout to denote a derivative with respect to proper

time. The quantities $\rho_b = \rho_b(t)$ and $P_b = P_b(t)$ are the total density and pressure of the constituents of the universe, respectively. The Friedmann equations determine the time evolution of the scale factor a and therefore describe the global expansion or contraction of the universe.

The study of cosmological structure formation requires an understanding of how small initial perturbations about the homogeneous and isotropic cosmology evolve with time. In general, the evolution equations for the perturbations are obtained by applying perturbation theory to the Einstein field equations; for a flavour of the various approaches see, for example: Lifshitz (1946), Hawking (1966), Bardeen (1980), Kodama and Sasaki (1984, 1987), Bruni *et al* (1992), Mukhanov *et al* (1992). However, if we assume that the length scale of the perturbations is much smaller than the Hubble radius then a Newtonian treatment of the perturbations is expected to be valid (e.g. Peebles 1980). Throughout this paper we will consider perturbations in the collisionless cold dark matter (CDM) distribution only. In other words, we are assuming that the distributions of all the other constituents of the universe (baryons, etc.) are unperturbed.

2.1. The fluid approach

In the Newtonian limit, the dynamical equations governing the evolution of fluctuations in the CDM distribution in an expanding universe can be written in the form:

$$\frac{\partial \mathbf{v}}{\partial t} + H\mathbf{v} + \frac{1}{a}(\mathbf{v} \cdot \nabla_{\mathbf{x}})\mathbf{v} + \frac{1}{a}\nabla_{\mathbf{x}}\Phi = 0, \quad (5)$$

$$\frac{\partial \delta}{\partial t} + \frac{1}{a}\nabla_{\mathbf{x}} \cdot [(1 + \delta)\mathbf{v}] = 0, \quad (6)$$

$$\nabla_{\mathbf{x}}^2\Phi - 4\pi G a^2 \rho_{b,d} \delta = 0, \quad (7)$$

where $\mathbf{x} = \mathbf{x}(t)$ are comoving coordinates, related to physical coordinates \mathbf{r} via $\mathbf{r} = a\mathbf{x}$. Here the scale factor has been normalized so that its present value $a_0 = 1$. The peculiar velocity field $\mathbf{v} = \mathbf{v}(\mathbf{x}, t)$ is defined by $\mathbf{v} = a\dot{\mathbf{x}}$ and the potential $\Phi = \Phi(\mathbf{x}, t)$ is the peculiar Newtonian gravitational potential. The density contrast $\delta = \delta(\mathbf{x}, t)$ is of the form $\delta = \rho/\rho_{b,d} - 1$ where $\rho = \rho(\mathbf{x}, t)$ is the CDM density field and $\rho_{b,d} = \rho_{b,d}(t)$ is the CDM density in the homogeneous and isotropic background cosmology described by the metric (1).

2.2. Linear perturbation theory

In the standard picture of large-scale structure formation the initial CDM distribution is almost homogeneous except for the presence of small fluctuations ($\delta \ll 1$) of primordial origin. The gravitational amplification of these perturbations can be followed at early times by linearizing the fluid equations; in other words we perturb the physical fluid quantities \mathbf{v} , δ and Φ about their value in the homogeneous background and keep only

first-order terms. It is straightforward to derive the PDE

$$\frac{\partial^2 \delta}{\partial t^2} + 2H \frac{\partial \delta}{\partial t} - 4\pi G \rho_{b,d} \delta = 0 \quad (8)$$

from the linearized Euler, continuity and Poisson equations. This equation describes the linear growth of fluctuations in the CDM density field. The general solution to (8) is of the form

$$\delta = AD_+ + BD_-, \quad (9)$$

where $A = A(\mathbf{x})$, $B = B(\mathbf{x})$ are functions to be determined and $D_+ = D_+(t)$, $D_- = D_-(t)$ are the so-called linear growth and decay factors respectively. It is customary to ignore the decaying mode as it is only the growing mode that is responsible for the formation of cosmic structure. Upon neglecting the decaying mode the linearized continuity equation can be inverted to give

$$\delta = -\frac{1}{ag} \nabla_{\mathbf{x}} \cdot \mathbf{v}, \quad (10)$$

where the function $g = g(t)$ is defined by

$$g = \frac{\dot{D}_+}{D_+}. \quad (11)$$

Inserting (10) into the linearized Poisson equation yields the following expression for the peculiar velocity \mathbf{v} :

$$\mathbf{v} = -\frac{g}{4\pi G a \rho_{b,d}} \nabla_{\mathbf{x}} \Phi + \mathbf{C}, \quad (12)$$

where $\mathbf{C} = \mathbf{C}(\mathbf{x}, t)$ is a function to be determined and $\nabla_{\mathbf{x}} \cdot \mathbf{C} = 0$. It is immediately clear from (12) that the velocity flow associated with the growing mode is irrotational in the linear regime. The flow will in fact remain irrotational as long as Kelvin's circulation theorem holds. However, in the case of a collisionless medium such as CDM, Kelvin's theorem breaks down when shell-crossing occurs, if the fluid velocity is subsequently defined as an average over the velocities of the different streams passing through the caustic. Vorticity can then be generated in collapsing regions and the fluid flow will no longer be globally irrotational.

We now briefly discuss the results of LPT for two special cases that are relevant from the point of view of this paper:

A static CDM-dominated universe with a cosmological constant. In order for the universe to be static we require $\ddot{a} = \dot{a} = 0$. The scale factor is then constant $a = a_0 = 1$. It follows from the Friedmann equations that $\Lambda = 4\pi G \rho_{b,d}$ and, since $\rho_{b,d} > 0$, the universe must be closed. Upon noting that $H = 0$ in a static universe, we find from (8) that the linear growth factor is given by

$$D_+ = \exp\left(\frac{t - t_i}{\tau}\right), \quad (13)$$

where t_i is some initial time and $\tau = 1/\sqrt{\Lambda}$ is the characteristic time-scale for the gravitational collapse of a density fluctuation. The function $g \equiv 1/\tau$.

An expanding spatially-flat CDM-dominated universe. In this case $H = 2/3t$, $4\pi G\rho_{\text{b,d}} = 2/3t^2$ and it follows from (8) that the linear growth factor is of the form

$$D_+ = \left(\frac{t}{t_i}\right)^{2/3}. \quad (14)$$

The function $g \equiv 2/3t$. It is evident from (14) that, in an expanding spatially-flat CDM-dominated universe, the growth rate of density perturbations is considerably less than in a static universe (13). This is due to the Hubble drag induced by the expansion of the universe.

The linearized fluid approach we have described here is relatively simple and also relatively reliable. It does, however, suffer from a number of shortcomings. Firstly, as mentioned previously, LPT does not guarantee a positive density field at all times. If, as is the case in standard cosmological models, the initial distribution function of density fluctuations is symmetric, the presence of evolved regions with $\delta \gg 1$ (galaxies or clusters) necessarily implies the existence of regions with negative matter density. This is a consequence of the fact that in LPT the symmetry of distribution function is preserved while the variance grows proportional to a^2 . Secondly, the fluid description applies only to cold material. While this may be a good approximation for CDM-dominated universes, the baryonic and neutrino components that are known to exist require a more complete description; for these we should solve the Boltzmann equation for the full phase-space distribution function. The third and final shortcoming of this approach is that we assume that there is a single fluid velocity at every Eulerian position. This will not be the case when the trajectories of fluid elements cross. Again, a full phase-space description must be employed to remedy this deficiency.

2.3. The Zeldovich approximation

The Zeldovich approximation (Zeldovich 1970) provides a simple means of following the evolution of cosmological perturbations into the quasi-linear regime $\delta \sim 1$. The Zeldovich approximation has the form:

$$\mathbf{x} = \mathbf{q} + D_+ \mathbf{s}, \quad (15)$$

where $\mathbf{x} = \mathbf{x}(\mathbf{q}, t)$ is the comoving Eulerian coordinate at time t of a particle labelled by a comoving Lagrangian coordinate \mathbf{q} . The function D_+ is the linear growth factor introduced previously. The vector field $\mathbf{s} = \mathbf{s}(\mathbf{q})$ is time-independent and is related to the initial velocity perturbation. The continuity condition $\rho d^3 \mathbf{x} = \rho_{\text{b,d}} d^3 \mathbf{q}$ can be used to construct an expression for the CDM density field in Eulerian space:

$$\delta = \frac{1}{|J|} - 1, \quad (16)$$

where $|J|$ is the Jacobian determinant of the mapping (15) between Lagrangian and Eulerian coordinates. A useful property of the Zeldovich approximation from the point

of view of this paper is that it is exact in one-dimension up until shell-crossing occurs. When particle trajectories cross the mapping from \mathbf{q} to \mathbf{x} is no longer unique and $|J|$ becomes zero. The density field then becomes singular and the Zeldovich approximation approximation breaks down. There are extensions to the Zeldovich approximation that overcome this problem; for example, the adhesion approximation (Gurbatov *et al* 1989). This method, together with other methods of its ilk, share some of the attractive features of the wave-mechanical approximation we now describe.

2.4. The wave-mechanical approach

The wave-mechanical approach to the study of large-scale structure formation was first suggested in a seminal paper by Widrow and Kaiser (1993). It involves rewriting the usual fluid equations of motion in the form of a non-linear Schrödinger equation coupled to a Poisson equation describing the action of gravity. The Schrödinger equation governs the evolution of a (complex) scalar field that can be thought of as representing CDM. We now outline the wave-mechanical theory in both static and expanding universes.

2.4.1. The wave-mechanical approach in a static universe In a static universe the background coordinates are no longer expanding ($H = 0$) and the scale factor $a = a_0 = 1$ is constant. The comoving coordinate \mathbf{x} and peculiar velocity $\mathbf{v} = \dot{\mathbf{x}}$ then coincide with the physical coordinate \mathbf{r} and physical velocity $\mathbf{u} = \dot{\mathbf{r}}$, respectively. The relevant fluid equations describing the evolution of fluctuations in the CDM distribution are then:

$$\frac{\partial \mathbf{v}}{\partial t} + (\mathbf{v} \cdot \nabla_{\mathbf{x}}) \mathbf{v} + \nabla_{\mathbf{x}} \Phi = 0, \quad (17)$$

$$\frac{\partial \rho}{\partial t} + \nabla_{\mathbf{x}} \cdot (\rho \mathbf{v}) = 0, \quad (18)$$

$$\nabla_{\mathbf{x}}^2 \Phi - 4\pi G(\rho - \rho_{\text{b,d}}) = 0. \quad (19)$$

In the linear regime, we have seen that the velocity flow associated with the growing mode is irrotational and that this will remain the case as long as there is no shell-crossing. We can then define a velocity potential $\varphi = \varphi(\mathbf{x}, t)$ via $\mathbf{v} = -\nabla_{\mathbf{x}} \varphi$. Upon integrating the Euler equation (17) we obtain the Bernoulli equation

$$\frac{\partial \varphi}{\partial t} - \frac{1}{2} |\nabla_{\mathbf{x}} \varphi|^2 - \Phi = 0. \quad (20)$$

The Bernoulli equation (20) and the continuity equation (18) can be combined by performing a *Madelung transformation* (Madelung 1926) of the form

$$\psi = \sqrt{\rho} \exp\left(\frac{-i\varphi}{\nu}\right), \quad (21)$$

where $\psi = \psi(\mathbf{x}, t)$ and ν is a real parameter with dimensions of $L^2 T^{-1}$. Applying the Madelung transformation leads to the following coupled Schrödinger-Poisson system:

$$i\nu \frac{\partial \psi}{\partial t} = \left[-\frac{\nu^2}{2} \nabla_{\mathbf{x}}^2 + \Phi + \mathcal{P} \right] \psi, \quad (22)$$

$$\nabla_{\mathbf{x}}^2 \Phi - 4\pi G(|\psi|^2 - \rho_{\text{b,d}}) = 0, \quad (23)$$

where $\mathcal{P} = \mathcal{P}(\mathbf{x}, t)$ is the so-called *quantum pressure* term, given by

$$\mathcal{P} = \frac{\nu^2}{2} \frac{\nabla_{\mathbf{x}}^2 |\psi|}{|\psi|}. \quad (24)$$

Historically this term has usually arisen in attempts to find a hydrodynamical interpretation of quantum mechanics. If we neglect the quantum pressure term for the moment then we are left with the linear Schrödinger equation

$$i\nu \frac{\partial \psi}{\partial t} = \left[-\frac{\nu^2}{2} \nabla_{\mathbf{x}}^2 + \Phi \right] \psi. \quad (25)$$

Inserting the Madelung transformation into (25) yields the usual continuity equation and a modified Bernoulli equation of the form

$$\frac{\partial \varphi}{\partial t} - \frac{1}{2} |\nabla_{\mathbf{x}} \varphi|^2 - \Phi + \mathcal{P} = 0, \quad (26)$$

and so the quantum pressure term appears in the classical fluid equations. In the present context the quantum pressure term represents an unwanted term in the fluid approach arising from our approximate description of a purely classical system in terms of wave-mechanics. The above comments suggest that we can drop the quantum pressure term from the non-linear Schrödinger equation (22) and include it in the Bernoulli equation instead; this is the approach that we will adopt throughout this paper.

The parameter ν appears in the Schrödinger equation in a manner analogous to the Planck constant in real quantum mechanics. The system we are considering here is entirely classical, so ν is treated as an adjustable parameter that controls the spatial resolution via a de Broglie-like relation. It is also plays a similar role to the viscosity parameter that appears in the adhesion approximation and which transforms the Euler equation into the *Burgers equation*. This is due to the fact that the Madelung transformation we employ here is mathematically related to the Hopf-Cole transformation needed to solve the Burgers equation; see Gurbatov *et al* (1989) for a further discussion of this point. For the behaviour of our fluid to be entirely classical, we require ν to be as small as possible in which case we intuitively expect the quantum pressure term to be negligible. However, as we shall see later, there are mathematical pitfalls one can fall into if one just assumes that ν can be taken infinitesimally small throughout.

Although this transformation of a purely classical problem into one involving quantum mechanics may appear strange, some advantages are immediately apparent. Given a solution ψ of the Schrödinger-Poisson system, the CDM density field ρ and velocity potential φ can be calculated from the phase and amplitude of the wavefunction

respectively. Since $\rho = |\psi|^2$ the wave-mechanical formalism guarantees a matter density that is everywhere positive. Moreover, this approach provides an elegant description of both the density and velocity fields in a single complex function. No singularities occur in the wavefunction at any time and so shell-crossing does not lead to the formation of singularities in the density field as in the Zeldovich approximation. What happens in effect is that the quantum nature of the description smears out particle trajectories; when particles are described in terms of wave packets they have a finite spatial extent. Particle trajectories still cross, but nothing diverges when this occurs.

The one remaining deficiency of the other approximation schemes that lingers in this one is that we have still assumed that there is a single fluid velocity at each point. This is not an intrinsic problem to do with the wave-mechanical formalism, but is instead a consequence of the very simple Madelung form of the wavefunction we have used. Widrow and Kaiser (1993) showed that in fact one can deploy more sophisticated representations of the wave function, such as the coherent state formalism of Husimi (1940), that allow for multi-streaming. With such an approach the Schrödinger equation can be used to follow the full Vlasov evolution of the phase-space distribution function beyond the laminar flow regime; see, for example, Skodje *et al* (1989). These extensions are beyond the scope of this paper.

2.4.2. The wave-mechanical approach in an expanding universe In an expanding universe it is convenient to rewrite the fluid equations (5), (6) and (7) in the alternative form:

$$\frac{\partial \mathbf{U}}{\partial a} + (\mathbf{U} \cdot \nabla_{\mathbf{x}}) \mathbf{U} + \left(\frac{2}{a} + \frac{\ddot{a}}{\dot{a}^2} \right) \mathbf{U} + \nabla_{\mathbf{x}} \Theta = 0, \quad (27)$$

$$\frac{\partial \delta}{\partial a} + \nabla_{\mathbf{x}} \cdot [(1 + \delta) \mathbf{U}] = 0, \quad (28)$$

$$\nabla_{\mathbf{x}}^2 \Theta - \frac{3\Omega_d}{2a^2} \delta = 0. \quad (29)$$

where the comoving velocity field $\mathbf{U} = \mathbf{U}(\mathbf{x}, a)$ is defined by $\mathbf{U} = d\mathbf{x}/da$ and is related to the peculiar velocity field by $\mathbf{v} = a\dot{a}\mathbf{U}$. The field $\Theta = \Theta(\mathbf{x}, a)$ is a scaled peculiar gravitational potential: $\Theta = \Phi/a^2\dot{a}^2$. The CDM density parameter $\Omega_d = \Omega_d(a)$ has been introduced and is given by $\Omega_d = 8\pi G\rho_{b,d}/3H^2$.

As before, we define a comoving velocity potential $\phi = \phi(\mathbf{x}, a)$ via $\mathbf{U} = -\nabla_{\mathbf{x}}\phi$. The Euler equation (27) can then be integrated once to obtain the Bernoulli equation

$$\frac{\partial \phi}{\partial a} - \frac{1}{2} |\nabla_{\mathbf{x}}\phi|^2 - \mathcal{V} = 0, \quad (30)$$

where the effective potential $\mathcal{V} = \mathcal{V}(\mathbf{x}, a)$ depends on both the comoving velocity potential and the gravitational potential:

$$\mathcal{V} = \Theta - \left(\frac{2}{a} + \frac{\ddot{a}}{\dot{a}^2} \right) \phi. \quad (31)$$

In light of the discussion of the quantum pressure term in the previous section, we modify the Bernoulli equation (30) by adding a quantum pressure term $\mathcal{P} = \mathcal{P}(\mathbf{x}, a)$ of the form

$$\mathcal{P} = \frac{\nu^2}{2} \frac{\nabla_{\mathbf{x}}^2 \sqrt{(1 + \delta)}}{\sqrt{(1 + \delta)}}, \quad (32)$$

which gives

$$\frac{\partial \phi}{\partial a} - \frac{1}{2} |\nabla_{\mathbf{x}} \phi|^2 - \mathcal{V} + \mathcal{P} = 0. \quad (33)$$

Applying the Madelung transformation

$$\psi = \sqrt{(1 + \delta)} \exp\left(\frac{-i\phi}{\nu}\right) \quad (34)$$

to the Bernoulli equation (33) and the continuity equation (28) yields the following Schrödinger-Poisson system:

$$i\nu \frac{\partial \psi}{\partial a} = \left(-\frac{\nu^2}{2} \nabla_{\mathbf{x}}^2 + \mathcal{V}\right) \psi, \quad (35)$$

$$\nabla_{\mathbf{x}}^2 \left[\mathcal{V} - \left(\frac{2}{a} + \frac{\ddot{a}}{a^2}\right) \nu \arg(\psi) \right] - \frac{3\Omega_d}{2a^2} (|\psi|^2 - 1) = 0, \quad (36)$$

where $\psi = \psi(\mathbf{x}, a)$ and the parameter ν now has dimensions of L^2 . The coupled Schrödinger-Poisson system describes the evolution of the wavefunction ψ for a general homogeneous and isotropic expanding background cosmology. However, an interesting special case arises when the universe is assumed to be spatially-flat and CDM-dominated (i.e. $\Omega_d = 1$). It is straightforward to show from (12) that, in this case, $\phi = 2a\Theta/3$ in the linear regime. This relation will remain valid as long as Kelvin's circulation theorem is not violated, i.e. into the quasi-linear regime. If we assume that ϕ and Θ are related in this manner then it is immediately clear from (31) that the effective potential \mathcal{V} is identically zero. This is an important point to note since the Schrödinger equation (35) then reduces to the exactly-solvable free-particle Schrödinger equation

$$i\nu \frac{\partial \psi}{\partial a} = -\frac{\nu^2}{2} \nabla_{\mathbf{x}}^2 \psi, \quad (37)$$

and the Poisson equation (36) becomes

$$\nu \nabla_{\mathbf{x}}^2 [\arg(\psi)] + \frac{1}{a} (|\psi|^2 - 1) = 0. \quad (38)$$

3. Examples of one-dimensional gravitational collapse

In this section we apply the wave-mechanical method to simple examples of one-dimensional gravitational collapse. More specifically, we consider the evolution of one-dimensional sinusoidal density perturbations in both static and expanding universes. We describe how to compare the wave-mechanical approximation with the established linearized fluid approach and Zeldovich approximation in each case. The reason for studying such simple examples is the hope that it will give us a clear insight into how the wave-mechanical approach behaves in a cosmological setting and, in particular, the role of the parameter ν and the quantum pressure term.

3.1. One-dimensional collapse in a static universe

We begin by considering a static CDM-dominated universe with a cosmological constant. Recall from our earlier discussion that, in this case, $\Lambda = 4\pi G\rho_{b,d}$ and the characteristic time-scale for the collapse of a density fluctuation is $\tau = 1/\sqrt{\Lambda}$. Our goal is to use the wave-mechanical approximation to follow the evolution of an initial one-dimensional density perturbation $\delta_i = \delta(x, t_i)$ of the form

$$\delta_i = \delta_a \cos\left(\frac{2\pi x}{d}\right), \quad (39)$$

where d is the period of the perturbation and $0 < \delta_a \leq 1$ to ensure that the initial CDM density field is everywhere positive. In the linear regime we have seen that the density perturbation grows according to $\delta = D_+ \delta_i$ where the linear growth factor $D_+ = \exp[(t - t_i)/\tau]$. The corresponding fluctuation in the gravitational potential associated with the growing mode is found from the linearized version of the Poisson equation (19):

$$\Phi = -\left(\frac{d}{2\pi\tau}\right)^2 \delta. \quad (40)$$

We use (40) as an external gravitational potential in the Schrödinger equation (22) so that the full one-dimensional Schrödinger equation we are aiming to solve is

$$i\nu \frac{\partial\psi}{\partial t} = \left[-\frac{\nu^2}{2} \frac{\partial^2}{\partial x^2} - \delta_a \left(\frac{d}{2\pi\tau}\right)^2 \exp\left(\frac{t - t_i}{\tau}\right) \cos\left(\frac{2\pi x}{d}\right) \right] \psi, \quad (41)$$

where $\psi = \psi(x, t)$. In order to solve this equation we must first specify the initial conditions. The linearized fluid approach provides an excellent description of gravitational instability at early times and so we use linear theory to construct an initial wavefunction $\psi_i = \psi(x, t_i)$ of the form

$$\psi_i = \sqrt{\rho_i} \exp\left(\frac{-i\varphi_i}{\nu}\right), \quad (42)$$

where $\rho_i = \rho(x, t_i)$ and $\varphi_i = \varphi(x, t_i)$ are the initial CDM density field and velocity potential respectively. We have $\rho_i = \rho_{b,d}(1 + \delta_i)$ with δ_i given by (39). The velocity

potential associated with the growing mode is found from the linearized version of the Bernoulli equation (20):

$$\varphi = -\frac{1}{\tau} \left(\frac{d}{2\pi} \right)^2 \delta, \quad (43)$$

and φ_i readily follows. The objective is now to solve the Schrödinger equation (41), with initial conditions given by (42), for the wavefunction ψ . However, it is not possible to find an exact solution of (41) and so we resort to approximate methods of solution.

In what follows we will restrict our attention to a large cubic volume of side length L equipped with periodic boundary conditions at each face. This is a construction commonly used in the study of cosmological structure formation in order to simplify calculations; the limit $L \rightarrow \infty$ can be taken as a final step. The initial density perturbation (39) we are considering is periodic with period d and, consequently, so is the gravitational potential Φ appearing in the Schrödinger equation (41). This suggests it will be convenient to divide our cubic volume into cells of side length d , i.e. set $L = Nd$, $N > 0$ an integer.

3.1.1. The Schrödinger equation with a time-independent external potential As a starting point, let us assume that the gravitational potential does not depend explicitly on time so that $\Phi = \Phi_i$ where

$$\Phi_i = - \left(\frac{d}{2\pi\tau} \right)^2 \delta_i. \quad (44)$$

This approximation holds at early times $t - t_i \ll \tau$ when the value of the linear growth factor $D_+ = \exp[(t - t_i)/\tau]$ is close to unity. The assumption of a fixed gravitational potential is somewhat reminiscent of the frozen potential approximation (Brainerd *et al* 1993, Bagla and Padmanabhan 1994). The full Schrödinger equation to be solved is then

$$i\nu \frac{\partial \psi}{\partial t} = \left[-\frac{\nu^2}{2} \frac{\partial^2}{\partial x^2} - \delta_i \left(\frac{d}{2\pi\tau} \right)^2 \cos \left(\frac{2\pi x}{d} \right) \right] \psi. \quad (45)$$

We have calculated a first-order approximate solution to (45) by using time-independent perturbation theory; see Appendix A.2 for details. The solution is found to be

$$\psi = \sum_n b_n \exp \left[\frac{-i(t - t_i)E_n}{\nu} \right] \phi_n, \quad (46)$$

where the energy eigenvalues are $E_n = \nu^2 k_n^2 / 2$ with $k_n = 2n\pi/L$ and $L = Nd$. The eigenfunctions $\phi_n = \phi_n(x)$ are of the form

$$\phi_n = \sum_{j=0}^1 \phi_n^{(j)}, \quad (47)$$

where $\phi_n^{(0)}$ are the eigenfunctions of the free-particle Schrödinger equation:

$$\phi_n^{(0)} = \frac{1}{L^{3/2}} \exp(ik_n x), \quad (48)$$

and

$$\phi_n^{(1)} = \frac{\delta_a}{16\pi^3\gamma^2} \phi_n^{(0)} \sum_{s=\pm 1} \frac{1}{s(k_n d + s\pi)} \exp\left(\frac{2is\pi x}{d}\right), \quad (49)$$

with $\gamma = \nu\tau/d^2$ a dimensionless parameter. The expansion coefficients b_n are found from

$$b_n = NL^2 \delta_{n,pN} \int_0^d \overline{\phi_n}(x) \psi_i(x) dx, \quad (50)$$

where ψ_i is given by (42) and p is an integer. The expansion coefficients are zero unless n is an integer multiple of N . The first-order perturbation expansion (47) of the eigenfunctions ϕ_n can be used to rewrite (46) as

$$\psi = \sum_{j=0}^1 \psi^{(j)}, \quad (51)$$

where $\psi^{(0)} = \psi^{(0)}(x, t)$ is of the form

$$\psi^{(0)} = \sum_n b_n \exp\left[\frac{-i(t - t_i)E_n}{\nu}\right] \phi_n^{(0)}, \quad (52)$$

and $\psi^{(1)} = \psi^{(1)}(x, t)$ is given by

$$\psi^{(1)} = \frac{\delta_a}{16\pi^3\gamma^2} \sum_n b_n \exp\left[\frac{-i(t - t_i)E_n}{\nu}\right] \phi_n^{(0)} \sum_{s=\pm 1} \frac{1}{s(k_n d + s\pi)} \exp\left(\frac{2is\pi x}{d}\right). \quad (53)$$

At any time of interest it is straightforward to calculate the CDM density field from the wavefunction ψ via

$$\delta = \frac{|\psi|^2}{\rho_{b,d}} - 1. \quad (54)$$

We wish to compare the performance of the wave-mechanical approach with that of linear theory and the Zeldovich approximation. The time-independent gravitational potential (44) is not a consistent solution of the linearized fluid equations, except at the initial time. However, by substituting (44) into the linearized Euler and continuity equations, we find that $\delta = D_+ \delta_i$ where the linear growth factor is modified to

$$D_+ = 1 + \frac{1}{2} \left(\frac{t^2 - t_i^2}{\tau^2} \right). \quad (55)$$

This is somewhat different from the usual exponential linear growth law one obtains upon letting the gravitational potential evolve with time. The CDM density field in the Zeldovich approximation is found from the expressions (15) and (16):

$$\delta = \frac{1}{(1 - D_+ \delta_i)} - 1, \quad (56)$$

where D_+ is given by (55) and we have used the linear relation (43) for the velocity potential to calculate the initial velocity perturbation in the Zeldovich approximation.

3.1.2. The Schrödinger equation with a time-dependent external potential We now allow the gravitational potential appearing in the Schrödinger equation to evolve with time according to the linear expression (40). The relevant Schrödinger equation to be solved is then (41), subject to the initial condition (42). We have used time-dependent perturbation theory to calculate a second-order approximate solution of the Schrödinger equation in this case; the details of the calculation are presented in Appendix A.3. We summarise the main results here for reference. The approximate solution $\psi = \psi(x, t)$ was found to be

$$\psi = \sum_{j=0}^2 \psi^{(j)}, \quad (57)$$

where $\psi^{(j)} = \psi^{(j)}(x, t)$. The zeroth-order term $\psi^{(0)}$ is

$$\psi^{(0)} = \sum_n a_n \exp \left[\frac{-i(t - t_i) E_n^{(0)}}{\nu} \right] \phi_n^{(0)}, \quad (58)$$

which is simply the solution of the free-particle Schrödinger equation ($\Phi = 0$). The first-order term $\psi^{(1)}$ is given by

$$\begin{aligned} \psi^{(1)} &= \frac{i\delta_a}{8\pi^2\gamma} \exp \left(\frac{t - t_i}{\tau} \right) \sum_n a_n \exp \left[\frac{-i(t - t_i) E_n^{(0)}}{\nu} \right] \phi_n^{(0)} \\ &\quad \times \sum_{s=\pm 1} \frac{1}{\zeta_{n,s}} \left(1 - \exp \left[\frac{-(t - t_i) \zeta_{n,s}}{\tau} \right] \right) \exp \left(\frac{2is\pi x}{d} \right), \end{aligned} \quad (59)$$

and the second-order term $\psi^{(2)}$ is

$$\begin{aligned} \psi^{(2)} &= - \left(\frac{\delta_a}{8\pi^2\gamma} \right)^2 \exp \left[\frac{2(t - t_i)}{\tau} \right] \sum_n a_n \exp \left[\frac{-i(t - t_i) E_n^{(0)}}{\nu} \right] \phi_n^{(0)} \\ &\quad \times \sum_{r=\pm 1} \sum_{s=\pm 1} \frac{1}{(\zeta_{n,s} + \eta_{n,r,s})} \exp \left[\frac{-(t - t_i) \zeta_{n,s}}{\tau} \right] \\ &\quad \times \left\{ \frac{1}{\zeta_{n,s}} \left(\exp \left[\frac{(t - t_i) \zeta_{n,s}}{\tau} \right] - 1 \right) \right. \\ &\quad \left. + \frac{1}{\eta_{n,r,s}} \left(\exp \left[\frac{-(t - t_i) \eta_{n,r,s}}{\tau} \right] - 1 \right) \right\} \exp \left[\frac{2i(r + s)\pi x}{d} \right]. \end{aligned} \quad (60)$$

Here the eigenfunctions $\phi_n^{(0)} = \phi_n^{(0)}(x)$ are as in (48) and the energy eigenvalues are $E_n^{(0)} = \nu^2 k_n^2 / 2$ with $k_n = 2n\pi/L$ and $L = Nd$. The parameter $\gamma = \nu\tau/d^2$ is dimensionless. The expansion coefficients a_n are found from

$$a_n = NL^2 \delta_{n,pN} \int_0^d \overline{\phi_n^{(0)}(x)} \psi_i(x) dx, \quad (61)$$

where p is an integer and ψ_i is given by (42). As before, the expansion coefficients are zero unless n is an integer multiple of N . Notice that the form of the free-particle eigenfunctions $\phi_n^{(0)}$ implies that the expansion coefficients can be calculated simply by taking the Fourier transform of the initial wavefunction. Finally, $\zeta_{n,s}$ and $\eta_{n,r,s}$ are given by

$$\zeta_{n,s} = 1 + 2is\pi\gamma(k_nd + s\pi) \quad (62)$$

and

$$\eta_{n,r,s} = 1 + 2ir\pi\gamma[k_nd + (r + 2s)\pi], \quad (63)$$

respectively.

The wavefunction (57) allows us to determine the CDM density field at any particular time by applying (54). In order to compare the wave-mechanical approach with LPT and the Zeldovich approximation, recall that the time-dependent gravitational potential (40) is a solution of the fluid equations in the linear regime. The growing mode of the linear density field is then $\delta = D_+\delta_i$ with $D_+ = \exp[(t - t_i)/\tau]$ as usual. Inserting D_+ into (56) gives the CDM density field in the Zeldovich approximation.

3.2. One-dimensional collapse in an expanding universe

We now turn our attention to the more relevant case of an expanding universe. For simplicity we will assume that the universe is spatially-flat and CDM-dominated. Our intention is again to use the wave-mechanical approach to follow the gravitational evolution of a one-dimensional sinusoidal density perturbation $\delta_i = \delta_i(x, a_i)$:

$$\delta_i = \delta_a \cos\left(\frac{2\pi x}{d}\right), \quad (64)$$

where d is the comoving period of the perturbation and $0 < \delta_a \leq 1$ as before. Recall that, in an expanding spatially-flat CDM-dominated universe, the relevant Schrödinger equation to be solved is the free-particle Schrödinger equation (37). In one-dimension this becomes

$$i\nu \frac{\partial\psi}{\partial a} = -\frac{\nu^2}{2} \frac{\partial^2\psi}{\partial x^2}, \quad (65)$$

where $\psi = \psi(x, a)$. To construct the initial wavefunction we again appeal to the results of linear theory. In a spatially-flat universe dominated by CDM the linear growth of the initial density fluctuation (64) is described by $\delta = D_+\delta_i$ with $D_+ = a/a_i$. From the linearized version of the continuity equation (28) it follows that the corresponding perturbation in the velocity potential is independent of time $\phi = \phi_i$ where

$$\phi_i = -\frac{1}{a_i} \left(\frac{d}{2\pi}\right)^2 \delta_i. \quad (66)$$

The initial wavefunction $\psi_i = \psi(x, a_i)$ is then

$$\psi_i = \sqrt{(1 + \delta_i)} \exp\left(\frac{-i\phi_i}{\nu}\right), \quad (67)$$

where δ_i and ϕ_i are given by (64) and (66) respectively. We now discuss the solution of the free-particle Schrödinger equation (65) subject to the initial conditions (67). As in the case of a static background, it is again convenient to consider a large cubic volume of comoving side length L equipped with periodic boundary conditions. The sinusoidal initial density perturbation (64) has a comoving period d and so we partition the cubic volume into cells of comoving side length d via $L = Nd$ where $N > 0$ is an integer.

3.2.1. Solution of the free-particle Schrödinger equation The solution to the free-particle Schrödinger equation in a static background was discussed in detail in Appendix A.1. Rather than repeating the calculation for the case of an expanding background, it suffices to note that we can simply replace the time coordinate t by the scale factor a in the solution obtained in Appendix A.1. We then find that the solution to the free-particle Schrödinger equation (65) is

$$\psi = \sum_n a_n \exp\left[\frac{-i(a - a_i)E_n^{(0)}}{\nu}\right] \phi_n^{(0)}, \quad (68)$$

where $E_n^{(0)} = \nu^2 k_n^2/2$ and $k_n = 2n\pi/L$ is now a comoving wavenumber. The eigenfunctions $\phi_n^{(0)}$ are of the form (48) and the expansion coefficients a_n are again determined from the Fourier transform of the initial wavefunction via

$$a_n = NL^2 \delta_{n,pN} \int_0^d \overline{\phi_n^{(0)}(x)} \psi_i(x) dx, \quad (69)$$

where p is an integer and ψ_i is given by (67). The coefficients are zero unless n is an integer multiple of N .

The wavefunction ψ can be used to calculate the CDM density field at any particular time via

$$\delta = |\psi|^2 - 1. \quad (70)$$

In order to assess the performance of the wave-mechanical approach, we compare (70) with the linear theory growth law $\delta = D_+ \delta_i$ and the Zeldovich approximation

$$\delta = \frac{1}{(1 - D_+ \delta_i)} - 1, \quad (71)$$

where $D_+ = a/a_i$ and we have made use of (66) in calculating the initial velocity perturbation.

4. Results and discussion

In the preceeding section we have applied the wave-mechanical approach to two examples of one-dimensional gravitational collapse in a static universe and an example of one-dimensional gravitational collapse in an expanding universe. In all cases we have considered an initial sinusoidal fluctuation in the CDM distribution:

$$\delta_i = \delta_a \cos\left(\frac{2\pi x}{d}\right). \quad (72)$$

In this section we show how this initial density perturbation evolves with time in the wave-mechanical approximation and compare our results with those obtained from the linearized fluid approach and the Zeldovich approximation. As we shall see, the performance of the wave-mechanical method depends strongly upon the free parameter ν and the quantum pressure term.

4.1. One-dimensional collapse in a static universe

We begin by discussing the the results obtained from using the wave-mechanical approach to model gravitational collapse in a static CDM-dominated universe with a cosmological constant. Recall that, as a starting point, we assumed the gravitational potential appearing in the Schrödinger equation was independent of time. The next step was then to allow the potential to evolve exponentially with time as in the linearized fluid approach. We now focus on each case in turn.

4.1.1. Time-independent gravitational potential In this simple situation the relevant Schrödinger equation to be solved was (45). A first-order approximate solution to this equation was found by applying time-independent perturbation theory; the resulting solution ψ is given by (46). The first-order term in the perturbation expansion of the wavefunction contains the dimensionless parameter $\gamma = \nu\tau/d^2$; once the amplitude of the initial density perturbation is specified, this parameter completely determines the behaviour of the wave-mechanical approximation. Notice that $\gamma \propto \nu$ and so we are free to use γ and ν interchangeably.

The CDM density field in the wave-mechanical approximation is obtained from the amplitude of the wavefunction via

$$\delta = \frac{|\psi|^2}{\rho_{b,d}} - 1. \quad (73)$$

The corresponding linear and Zeldovich approximation density fields are found from

$$\delta = \left[1 + \frac{1}{2} \left(\frac{t^2 - t_i^2}{\tau^2} \right) \right] \delta_i \quad (74)$$

and

$$\delta = \left\{ 1 - \left[1 + \frac{1}{2} \left(\frac{t^2 - t_i^2}{\tau^2} \right) \right] \delta_i \right\}^{-1} - 1, \quad (75)$$

respectively. It is then clear that shell-crossing occurs at a time $t = t_{\text{sc}}$ where

$$t_{\text{sc}} = \left[t_i^2 + 2\tau^2 \left(\frac{1}{\delta_a} - 1 \right) \right]^{1/2}. \quad (76)$$

For the rest of this paper we choose the amplitude of the initial density perturbation to be $\delta_a = 0.01$ for illustrative purposes. We follow the evolution from the initial time $t_i = 0$ up until the time of shell-crossing which, in the case at hand, is then $t_{\text{sc}}/\tau \approx 14.1$.

We now use the wave-mechanical approach to investigate the gravitational collapse of the initial density perturbation δ_i for several different choices of the parameter γ . This will give us some important insights into the nature of the wave-mechanical method. As a starting point we choose $\gamma = 0.003$. The plots in the left-hand column of figure 1 show how the wave-mechanical density field behaves as a function of time in this case. The LPT and Zeldovich approximation density fields are also shown for reference. The density field is periodic with period d by construction and so it is sufficient to plot the density field for x in the interval $[0, d]$ only.

A first point to note from figure 1(a) is that the initial wave-mechanical density field is very different from the initial sinusoidal density perturbation (72). In particular, the mean value of δ_i is not zero as it should be. As a result the wave-mechanical density field does not agree well with the LPT and Zeldovich approximation density fields at later times, as we can see from figure 1(b) and figure 1(c). To understand why the wave-mechanical approach performs poorly in this case, recall that the first-order perturbation expansion of the eigenfunctions ϕ_n appearing in the wavefunction ψ is

$$\phi_n = \sum_{j=0}^1 \phi_n^{(j)}, \quad (77)$$

where $\phi_n^{(0)}$ are the free-particle eigenfunctions (48) and $\phi_n^{(1)}$ is given by

$$\phi_n^{(1)} = \frac{\delta_a}{16\pi^3\gamma^2} \phi_n^{(0)} \sum_{s=\pm 1} \frac{1}{s(k_n d + s\pi)} \exp\left(\frac{2is\pi x}{d}\right). \quad (78)$$

In order for the perturbation expansion (77) to be valid we require the first-order term $\phi_n^{(1)}$ to be much smaller than the zeroth-order term $\phi_n^{(0)}$. However, $\phi_n^{(1)} \propto 1/\gamma^2$ and so, for small values of γ , we expect the first order term to be large relative to the zeroth-order term. Recall that the expansion coefficients b_n in the solution (46) of the Schrödinger equation are zero unless n is an integer multiple of N . If we assume that $n = pN$, p an integer, then $k_n d = 2p\pi$ and we find that $\phi_n^{(1)} \ll \phi_n^{(0)}$ if

$$\frac{\delta_a}{16\pi^4\gamma^2} \left| \sum_{s=\pm 1} \frac{1}{s(2p + s)} \exp\left(\frac{2is\pi x}{d}\right) \right| \ll 1. \quad (79)$$

Upon applying the triangle inequality we may rewrite this as

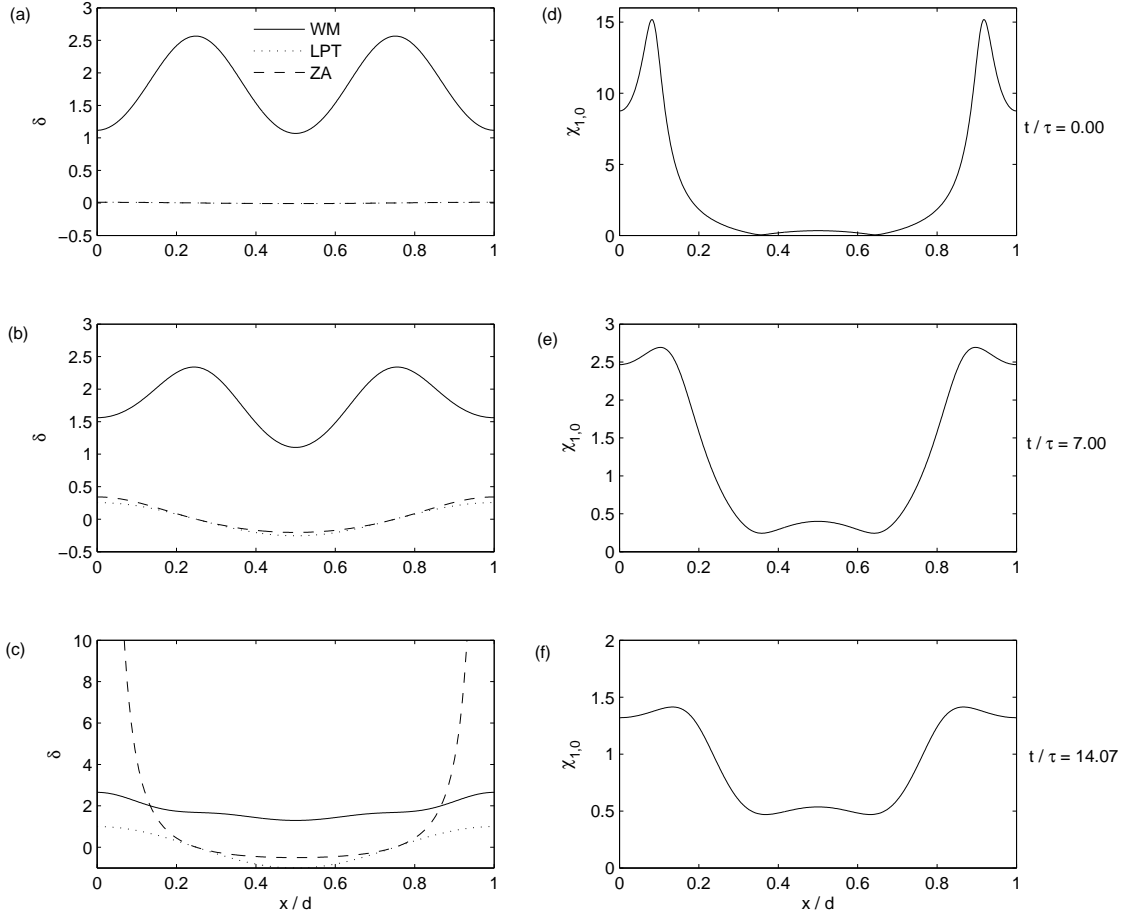


Figure 1. Time-evolution of an initially sinusoidal density perturbation in a static CDM-dominated universe with a cosmological constant. The amplitude of the initial density perturbation is $\delta_a = 0.01$. The left-hand plots show the density fields obtained from the first-order wave-mechanical approach with a time-independent gravitational potential (WM), the linearized fluid approach (LPT) and the Zeldovich approximation (ZA) at three different times. The parameter $\gamma = 0.003$ in the wave-mechanical approximation. The right-hand plots show the corresponding evolution of the ratio $\chi_{1,0}$ defined in the text.

$$\begin{aligned}
 \frac{\delta_a}{16\pi^4\gamma^2} \left| \sum_{s=\pm 1} \frac{1}{s(2p+s)} \exp\left(\frac{2is\pi x}{d}\right) \right| &\leq \frac{\delta_a}{16\pi^4\gamma^2} \sum_{s=\pm 1} \frac{1}{|2p+s|} \\
 &\leq \frac{\delta_a}{8\pi^4\gamma^2}, \tag{80}
 \end{aligned}$$

which immediately implies that we require

$$\gamma \gg \frac{1}{2\pi^2} \sqrt{\frac{\delta_a}{2}} \quad (81)$$

to guarantee $\phi_n^{(1)} \ll \phi_n^{(0)}$ for all values of n . Remember that $\delta_a = 0.01$ and so condition (81) gives $\gamma \gg 0.004$, approximately. This condition is not satisfied in the case $\gamma = 0.003$. As a result, we find that when the initial wavefunction ψ_i is expanded in terms of the eigenfunctions (77), the density field obtained from the amplitude of ψ_i does not match the true initial density perturbation. This disparity becomes increasingly worse if the value of γ is reduced further. We attempt to quantify this non-perturbative behaviour by considering the relative sizes of the zeroth and first-order terms in the perturbation expansion of the wavefunction:

$$\psi = \sum_{j=0}^1 \psi^{(j)}, \quad (82)$$

where $\psi^{(0)}$ and $\psi^{(1)}$ are given by (52) and (53) respectively. To do this we introduce a ratio $\chi_{1,0}$, defined by

$$\chi_{1,0} = \frac{|\psi^{(1)}|}{|\psi^{(0)}|}, \quad (83)$$

where we should have $\chi_{1,0} \ll 1$ for our perturbative solution to hold. The plots in the right-hand column of figure 1 show how $\chi_{1,0}$ behaves with time when $\gamma = 0.003$. It is evident that, as suspected, the nature of our system is indeed non-perturbative; at all times the first-order contribution $\psi^{(1)}$ to the wavefunction is certainly not negligible in comparison with $\psi^{(0)}$.

The preceding discussion suggests that the performance of the wave-mechanical approach will improve as the value of γ is increased. To investigate this we now consider $\gamma = 0.01$. The left-hand column of figure 2 shows the time-variation of the wave-mechanical density field in this case. To begin with, we can immediately see from figure 2(a) that the departure of the initial wave-mechanical density field from the true initial sinusoidal density field is less than when $\gamma = 0.003$ (figure 1). However, there is still a significant deviation, arising from the fact that (81) is not well satisfied.

The other plots in the left-hand column show that, as time proceeds, the wave-mechanical density field evolves in a similar manner to the linear theory and Zeldovich approximation density fields. Figure 2(b) demonstrates that the wave-mechanical approach agrees well with the other approximations at $t \approx t_{sc}/2$. At times close to shell-crossing (figure 2(c)) the Zeldovich approximation (which is exact in one-dimension) leads to large over-densities at $x = 0$ and $x = d$ which are not present in the wave-mechanical density field. However, in under-dense regions the wave-mechanical approach seems to provide a close match to the Zeldovich approximation.

It is also informative to look at how the ratio $\chi_{1,0}$ behaves when $\gamma = 0.01$. The time-evolution of $\chi_{1,0}$ is shown in the right-hand column of figure 2. It is obvious that the

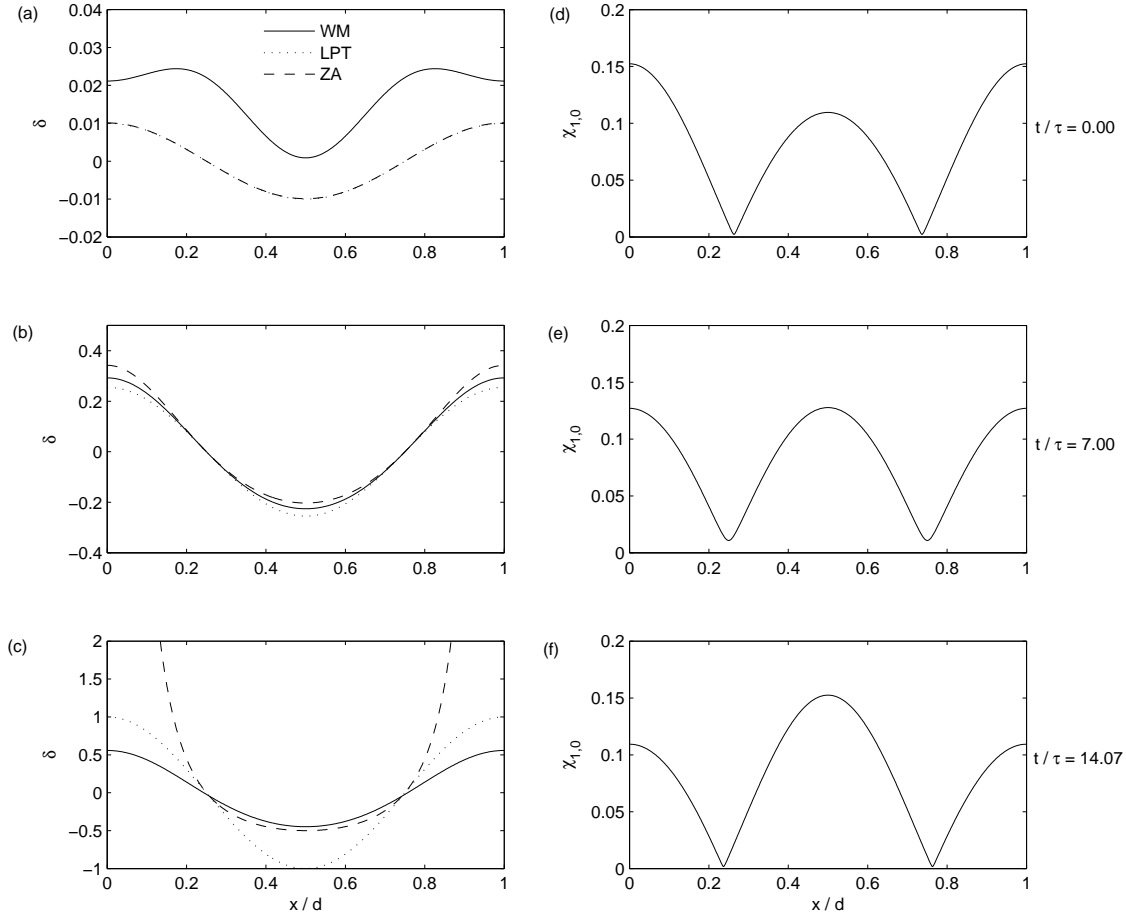


Figure 2. Time-evolution of an initially sinusoidal density perturbation in a static universe. The layout of the plots is as in figure 1; the only difference is that the parameter $\gamma = 0.01$ in the wave-mechanical approximation.

value of $\chi_{1,0}$ is consistently smaller than in the $\gamma = 0.003$ case and, importantly, $\chi_{1,0} < 1$ at all times. This signifies that $\psi^{(0)}$ is the dominant contribution to the perturbation expansion (82) as it should be.

The results shown in figure 2 do indeed seem to imply that the wave-mechanical approach performs considerably better as the value of γ is increased from $\gamma = 0.003$ to $\gamma = 0.01$. However, if we increase γ further we find that the wave-mechanical approximation exhibits unusual behaviour. The evolution of the wave-mechanical density field for $\gamma = 0.02$ is displayed in the left-hand column of figure 3. We can see from figure 3(a) that the initial wave-mechanical density field is now in much better agreement with the true initial sinusoidal density perturbation. Figure 3(b) shows that at $t \approx 2t_{\text{sc}}/3$ the wave-mechanical density field is behaving as anticipated (in the sense that the density is increasing in over-dense regions and decreasing in under-

dense regions), although the growth rate of the over-densities is again less in the wave-mechanical approach than in the other two approximation schemes. However, as the time approaches the time of shell-crossing, we find that the over-densities cease to grow in the wave-mechanical approximation and actually begin to decay. This is evident from a comparison of figure 3(b) with figure 3(c). This behaviour is counter-intuitive; the over-densities should continue to grow up until t_{sc} as in LPT and the Zeldovich approximation. We believe that this effect is due to the quantum pressure term.

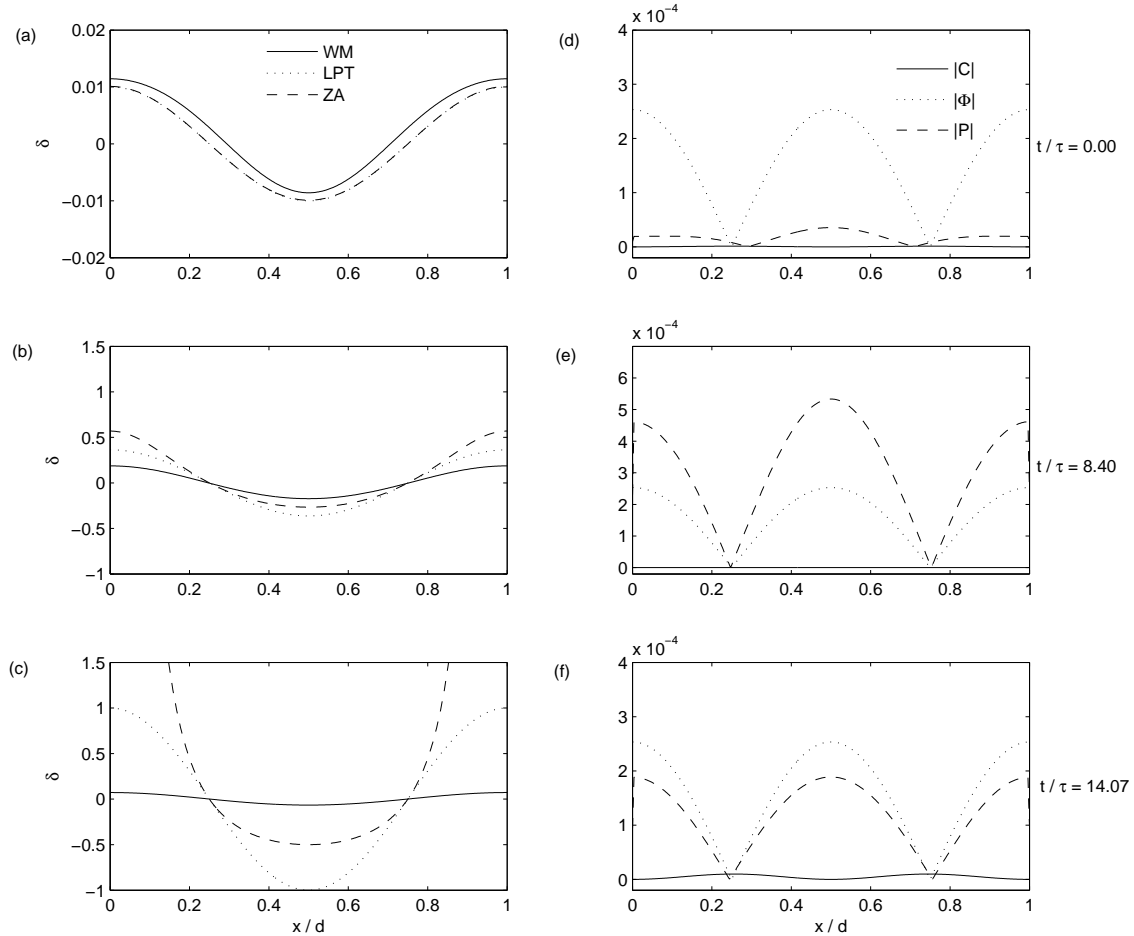


Figure 3. Time-evolution of an initially sinusoidal density perturbation in a static universe. The left-hand plots are as in figure 1, except that the parameter $\gamma = 0.02$ in the wave-mechanical approximation. The right-hand plots show the corresponding evolution of the magnitudes of the convective (C), gravitational potential (Φ) and quantum pressure (\mathcal{P}) terms, in units of d^2/τ^2 .

Recall that the quantum pressure term \mathcal{P} enters our formalism via the modified Bernoulli equation

$$\frac{\partial \varphi}{\partial t} + \mathcal{C} - \Phi + \mathcal{P} = 0, \quad (84)$$

where $\mathcal{C} = \mathcal{C}(x, t)$ is the convective term, defined in one-dimension by

$$\mathcal{C} = -\frac{1}{2} \left(\frac{\partial \varphi}{\partial x} \right)^2, \quad (85)$$

$\Phi = \Phi_i$ is the time-independent gravitational potential (44) and

$$\mathcal{P} = \frac{\nu^2}{2} \frac{1}{\sqrt{\rho}} \frac{\partial^2 \sqrt{\rho}}{\partial x^2}. \quad (86)$$

The quantum pressure $\mathcal{P} \propto \nu^2 \propto \gamma^2$ and so we expect γ to control the relative contribution of the quantum pressure term to (84). The plots in the right-hand column of figure 3 compare the time-variation of $|\mathcal{C}|$, $|\Phi|$ and $|\mathcal{P}|$. We can see that the gravitational potential is the dominant term at the initial time. However, as time passes, the quantum pressure term grows and eventually dominates the other two terms; see figure 3(e) and figure 3(f). As the quantum pressure term increases, the growth of the density perturbation in the wave-mechanical approach slows and eventually halts. The over-densities then begin to decay in an unphysical manner. This suggests that the quantum pressure term somehow acts to impede the growth of density perturbations in the wave-mechanical approximation.

This effect becomes more pronounced if we increase the value of γ further. Since $\mathcal{P} \propto \gamma^2$ we anticipate that an increase in γ will result in the quantum pressure term becoming more significant relative to the other two terms appearing in the Bernoulli equation (84). The left-hand column of figure 4 illustrates how the wave-mechanical density field behaves as a function of time when $\gamma = 1$. In this case, the density field simply oscillates about the mean value $\langle \delta \rangle = 0$ and there is no net growth of the initial density fluctuation. We find that this oscillatory behaviour persists for any $\gamma > 1$. The corresponding evolution of the terms $|\mathcal{C}|$, $|\Phi|$ and $|\mathcal{P}|$ is shown in the right-hand column of figure 4. It is immediately clear that the quantum pressure is indeed the dominant term appearing in (84) at all times (actually, the quantum pressure momentarily becomes zero as the density field passes through $\delta = 0$).

In this section we have examined in detail the behaviour of the wave-mechanical approximation with a time-independent gravitational potential for a range of values of the dimensionless parameter γ . We have found that, for values of $\gamma \sim 1$, the wave-mechanical density field simply oscillates between $\pm \delta_a$ and there is no growth of the initial density perturbation. In such cases the quantum pressure term is the dominant term appearing in the Bernoulli equation (84). It is interesting to note that gas pressure in a baryonic fluid causes a qualitatively similar effect (e.g. Coles and Lucchin 2002). If we were considering a baryonic fluid (rather than a fluid of pressureless CDM particles) then it would be necessary to account for the effects of gas pressure by including a classical pressure term in the Euler equation. Applying LPT to the fluid equations then yields a characteristic length scale (the *Jean's length*); any Fourier modes of the density field with a wavelength smaller than this Jean's length undergo damped oscillation rather than growth. In other words the classical pressure term causes the growth of baryon

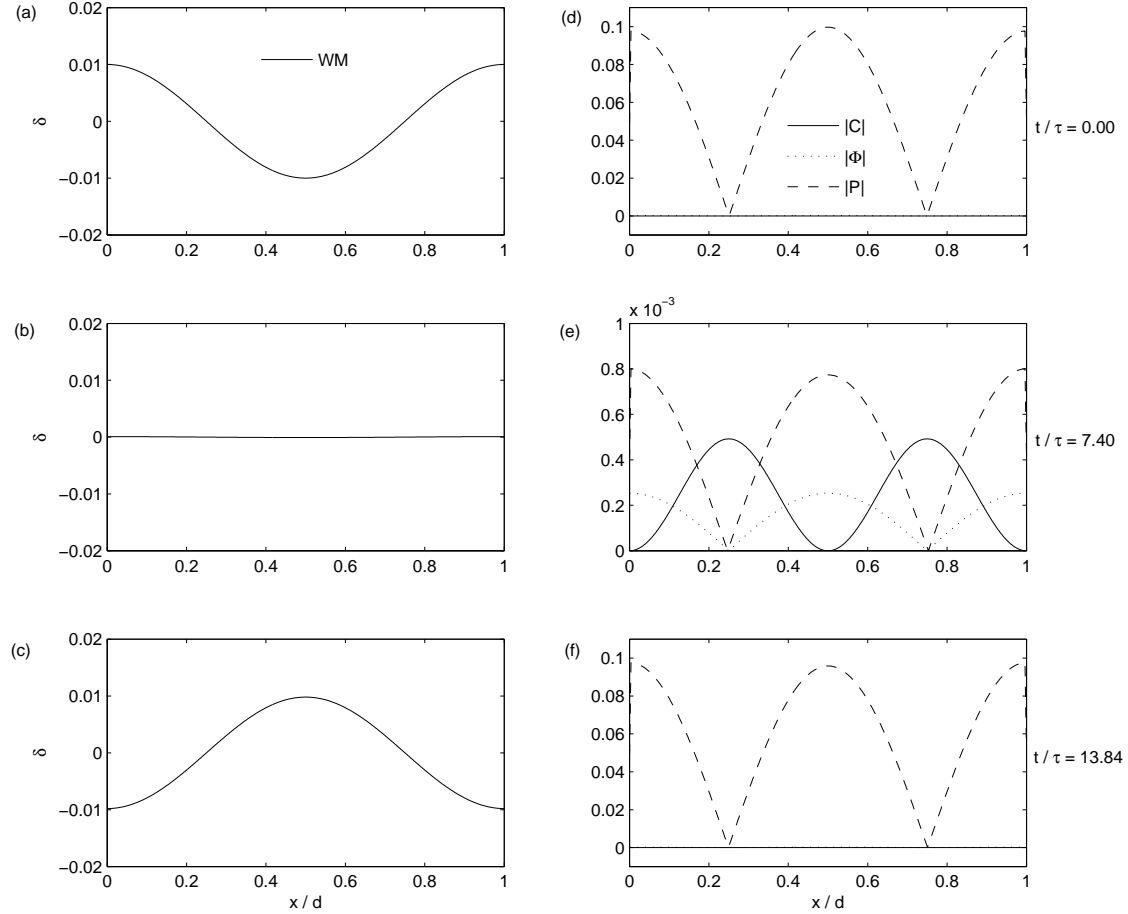


Figure 4. Time-evolution of an initially sinusoidal density perturbation in a static universe. The left-hand plots show the density field obtained from the first-order wave-mechanical approach with a time-independent gravitational potential (WM). The parameter $\gamma = 1$ in the wave-mechanical approximation. The right-hand plots are as in figure 3.

density perturbations to be impeded on scales smaller than the Jean's length. However, we must be careful not to directly compare the effects of the quantum pressure term to those of a classical pressure term as the origin and form of the two terms is very different. If we choose a smaller value of γ (such as $\gamma = 0.02$) then we find that the gravitational potential term in the Bernoulli equation dominates the quantum pressure term at early times. The wave-mechanical density field then behaves in a manner consistent with LPT and the Zeldovich approximation. However, the quantum pressure soon grows and the gravitational collapse of the density perturbation slows and eventually halts in the wave-mechanical approximation. The over-densities in the density field then begin to decay. It thus seems as if the quantum pressure term acts to inhibit the growth of density fluctuations in some way.

The quantum pressure term is proportional to γ^2 and so we anticipate the undesirable effects of this term should be negligible in the limit $\gamma \rightarrow 0$. Recall that we are particularly interested in this limit since we expect to recover the usual hydrodynamical equations from the Schrödinger equation. However, as we have seen, we cannot choose the value of γ to be arbitrarily small as this violates the validity condition (81) for our perturbative solution of the Schrödinger equation. As the value of γ is reduced, we find that the system becomes increasingly non-perturbative and the wave-mechanical approach performs poorly relative to the linearized fluid and Zeldovich approximations. This non-perturbative behaviour is somewhat reminiscent of the onset of turbulence in a classical fluid. It is interesting to speculate that small values of γ could be linked to some form of turbulent behaviour in our hydrodynamical description of quantum mechanics, especially when we realise that ν has dimensions of viscosity and that the dimensionless parameter $1/\gamma$ is very similar to the Reynold's number appearing in fluid mechanics. Turbulence in classical fluids is associated with the formation of vortices which obviously does not occur in one-dimensional systems. Nevertheless the analogy is compelling. A possible explanation is that very small values of γ involve large angular frequencies in the phase of the wavefunction (which is proportional to $1/\gamma$). To regain classical behaviour in the limit $\gamma \rightarrow 0$ the waves from which ψ is constructed must cancel exactly. Since the limit $\gamma \rightarrow 0$ involves waves of infinitely small wavelength, any finite perturbative calculation will find convergence impossible. A related but converse phenomenon arises in Eulerian fluids (i.e. fluids without intrinsic viscosity) when they are described in terms of a truncated spectrum (Cichowlas *et al* 2005).

To summarize, our first-order perturbative wave-mechanical approach with a time-independent gravitational potential is extremely sensitive to the parameter γ . On the one hand, we want to take the limit $\gamma \rightarrow 0$ so that the quantum pressure term is negligibly small and the usual fluid equations are recovered. On the other hand, the condition that our perturbative solution of the Schrödinger equation is valid requires $\gamma \gg 0.004$, approximately. There is clearly a conflict here. The best we can do is to choose a sufficiently small γ such that the quantum pressure is small enough not to cause the over-dense regions in the wave-mechanical density field to begin to decay in an unphysical manner. However, γ should also be large enough to satisfy the condition (81) as well as possible. In the example discussed above we find that the optimal value of γ is 0.01 (figure 2). Even in this case there is still a large discrepancy between the wave-mechanical approach and the Zeldovich approximation in over-dense regions at the time of shell-crossing. The results of the wave-mechanical approximation also differ significantly from those of LPT. However, the linearized fluid approach does lead to the formation of a region with $\delta < -1$ at shell-crossing; at least this problem is avoided in the wave-mechanical approach.

We should remember that a time-independent gravitational potential is not physically consistent (except at very early times) and so it is not surprising that the wave-mechanical approximation gives relatively poor results in this case. The main purpose of this simple example has been to highlight some of the properties of the wave-

mechanical approach and issues regarding perturbative solutions of the Schrödinger equation which, as we shall see, remain pertinent when the gravitational potential is allowed to evolve with time.

4.1.2. Time-dependent gravitational potential In the previous section we assumed the gravitational potential appearing in the Schrödinger equation did not depend on time. However, in the linear regime the gravitational potential grows exponentially with time in a static background. The natural path to follow is to incorporate this time-evolution of the gravitational potential into the Schrödinger equation as in section 3.1.2. In this situation the appropriate Schrödinger equation to be solved was (41); an approximate solution (57) to this equation was calculated by using second-order time-dependent perturbation theory. As in the time-independent case, the perturbative solution (57) depends on the dimensionless parameter $\gamma = \nu\tau/d^2$.

In the wave-mechanical approach the CDM density field is again determined from (73). However, the linear and Zeldovich approximation density fields are now given by

$$\delta = \exp\left(\frac{t - t_i}{\tau}\right)\delta_i \quad (87)$$

and

$$\delta = \left[1 - \exp\left(\frac{t - t_i}{\tau}\right)\delta_i\right]^{-1} - 1, \quad (88)$$

respectively. The time at which shell-crossing occurs is then $t_{sc} = t_i - \tau \ln(\delta_a)$ which, for $\delta_a = 0.01$ and $t_i = 0$, is $t_{sc}/\tau \approx 4.6$.

We have investigated the gravitational collapse of the initial sinusoidal density perturbation (72) using the wave-mechanical approximation with a time-dependent potential. As before, we have considered a range of different values of γ . To begin with we choose $\gamma = 0.015$. The left-hand column of figure 5 show the time-evolution of the wave-mechanical density field in this case. The LPT and Zeldovich approximation density fields are also shown for comparative purposes. It is immediately evident from figure 5(a) and figure 5(b) that the wave-mechanical density field provides a close match to the density field of the other approximation schemes up to $t \approx 2t_{sc}/3$. However, at times close to shell-crossing, an over-density appears at $x = d/2$ (i.e. where the gravitational potential is at a maximum) in the wave-mechanical density field. This is clearly not physical. To explain this, recall that the second-order perturbative solution to the Schrödinger equation is

$$\psi = \sum_{j=0}^2 \psi^{(j)}, \quad (89)$$

where $\psi^{(0)}$, $\psi^{(1)}$ and $\psi^{(2)}$ are given by (58), (59) and (60) respectively. We have that $\psi^{(1)} \propto 1/\gamma$ and $\psi^{(2)} \propto 1/\gamma^2$ and so, for small values of γ , we anticipate that these terms will be large compared to $\psi^{(0)}$. To check this, we again define a ratio

$$\chi_{j,0} = \frac{|\psi^{(j)}|}{|\psi^{(0)}|}, \quad (90)$$

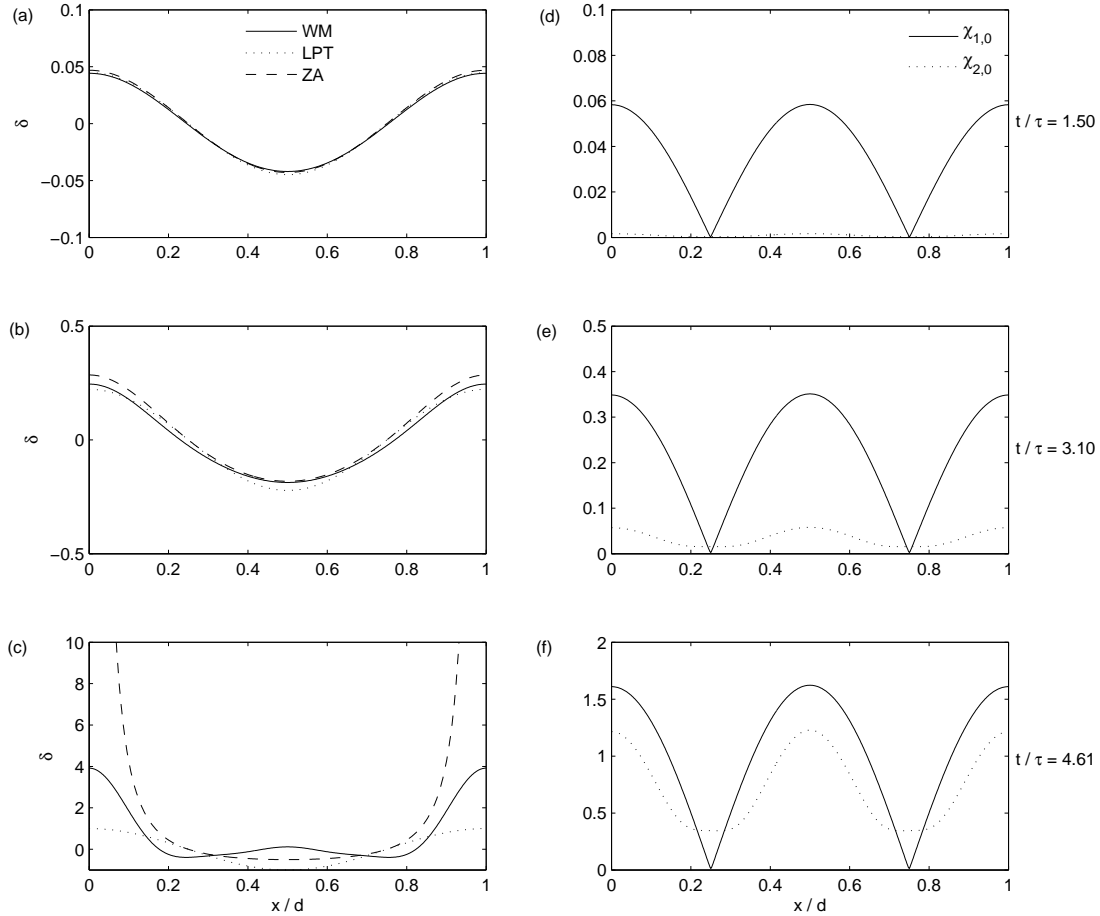


Figure 5. Time-evolution of an initially sinusoidal density perturbation in a static CDM-dominated universe with a cosmological constant. The amplitude of the initial density perturbation is $\delta_a = 0.01$. The left-hand plots show the density fields obtained from the second-order wave-mechanical approach with a time-dependent gravitational potential (WM), the linearized fluid approach (LPT) and the Zeldovich approximation (ZA) at three different times. The parameter $\gamma = 0.015$ in the wave-mechanical approximation. The right-hand plots show the corresponding evolution of the ratios $\chi_{1,0}$ and $\chi_{2,0}$ defined in the text.

with $j = 1, 2$. The ratios $\chi_{1,0}$ and $\chi_{2,0}$ are shown as functions of time in the right-hand column of figure 5. At early times $\chi_{1,0}$ and $\chi_{2,0}$ are both small as they should be. However, they both grow with time until, at $t \approx t_{sc}$, the first and second-order terms in the perturbation expansion of the wavefunction are comparable to the zeroth-order term. A general feature is that the first-order term initially grows at a faster rate than the second-order term, but as the time of shell-crossing approaches, the second-order term begins to grow very rapidly and is soon comparable to the first-order term. The false over-density at $x = d/2$ then develops, suggesting that this is due to

the non-perturbative behaviour of the system.

As in the previous section we intuitively expect our second-order perturbative solution of the Schrödinger equation to become more accurate as γ is made larger. Figure 6 illustrates the behaviour of wave-mechanical approximation when $\gamma = 0.02$. The plots in the left-hand column show the time-variation of the wave-mechanical density field in this case. It is clear from figure 6(a) and figure 6(b) that, as before, the wave-mechanical approach is in good agreement with the linearised fluid and Zeldovich approximations for times up to $t \approx 2t_{\text{sc}}/3$. Figure 6(c) shows that the wave-mechanical density field is also well behaved at $t \approx t_{\text{sc}}$ in this case; in particular, there is no unphysical over-density at $x = d/2$. Notice that the wave-mechanical approximation leads to the formation of larger over-densities than LPT, but it still does not provide a close match to the Zeldovich approximation in the over-dense regions at late times. However, the wave-mechanical density field does agree well with the Zeldovich approximation in under-dense regions.

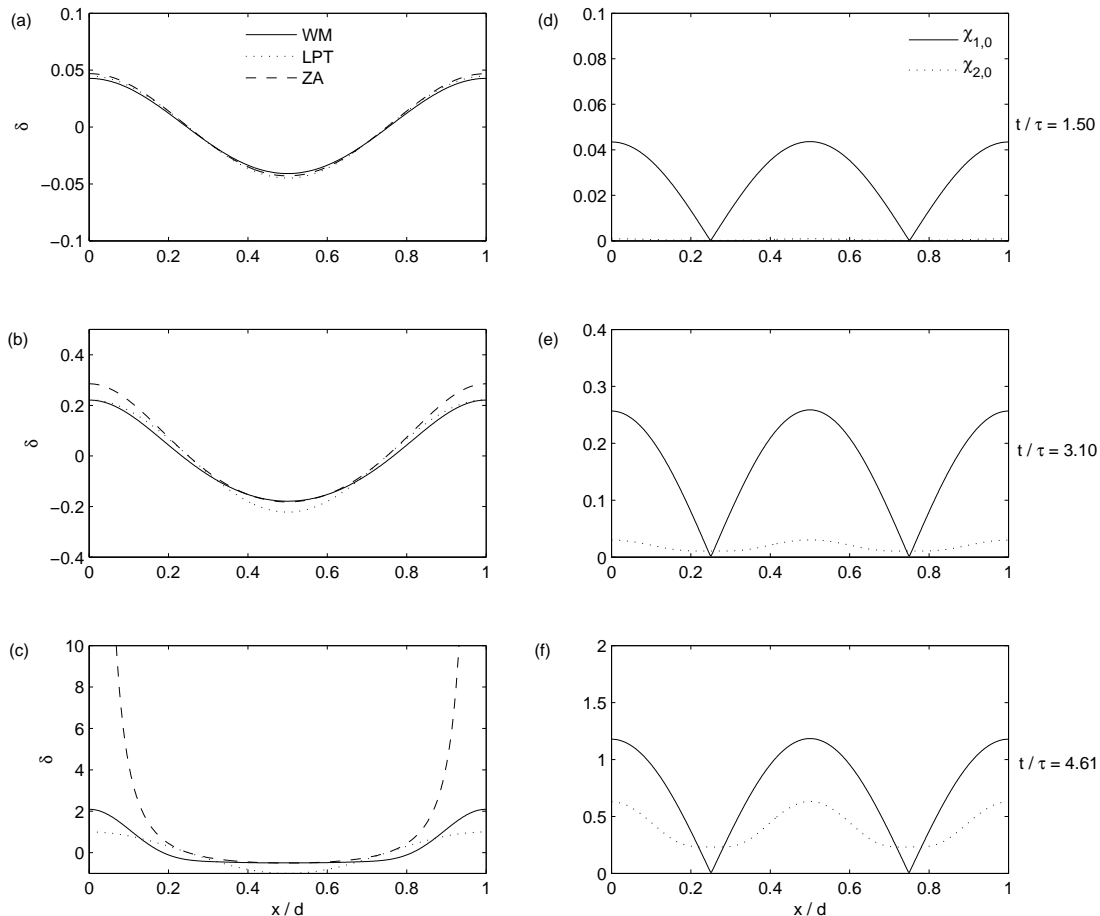


Figure 6. Time-evolution of an initially sinusoidal density perturbation in a static universe. The layout of the plots is as in figure 5; the only difference is that the parameter $\gamma = 0.02$ in the wave-mechanical approximation.

The plots in the right-hand column of figure 6 display the corresponding evolution of the ratios $\chi_{1,0}$ and $\chi_{2,0}$ for $\gamma = 0.02$. As suspected, the values of these ratios are consistently less than in the $\gamma = 0.015$ case. This signifies that the first and second-order terms in the perturbation expansion of the wavefunction are not as large relative to the zeroth-order term when $\gamma = 0.02$. However, at $t \approx t_{sc}$, the first and second-order terms are again becoming comparable to the zeroth-order term; if we use the wave-mechanical approach to follow the gravitational evolution of the density fluctuation past shell-crossing we indeed find that an unwanted over-density develops at $x = d/2$.

The wave-mechanical approximation exhibits interesting behaviour when the value of γ is increased to $\gamma = 0.1$. The evolution of the wave-mechanical density field in this case is shown in the left-hand column of figure 7. By comparing figure 7(a) with figure 7(b) we can see that the initial over-densities begin to decay rather than grow. However, at $t \approx t_{sc}/3$ the decay slows and halts and the over-densities then begin to grow in the usual fashion up to $t \approx t_{sc}$. Since the over-densities only begin to grow at $t \approx t_{sc}/3$ in the wave-mechanical approximation, the final wave-mechanical density field is considerably smoother than the density fields obtained from LPT and the Zeldovich approximation.

The rather strange behaviour of the wave-mechanical density field again appears to be due to the quantum pressure term. The magnitudes of the three terms \mathcal{C} , Φ and \mathcal{P} appearing in the Bernoulli equation (84) are plotted as functions of time in the right-hand column of figure 7. The quantum pressure term is clearly the dominant term at the initial time when the initial over-densities begin to decay in the wave-mechanical approximation. However, the gravitational potential grows exponentially with time and, at $t \approx t_{sc}/3$, dominates over the quantum pressure and convective terms. This corresponds to the time when the over-densities cease to decay and begin to grow instead. The gravitational potential remains the dominant term up until shell-crossing occurs.

In the time-independent example of the previous section we saw that, for $\gamma \sim 1$, the quantum pressure term is the dominant term in the Bernoulli equation. The wave-mechanical density field then simply oscillates between $\pm\delta_a$; see figure 4. We find that the same behaviour is observed in the time-dependent case for $\gamma \sim 1$. The quantum pressure term remains the dominant term at all times even though the gravitational potential is now increasing exponentially with time. As before, the wave-mechanical density field oscillates about $\langle \delta \rangle = 0$ and there is no overall growth of the initial density fluctuation.

In this section we have studied the wave-mechanical approach with a time-dependent gravitational potential. We have explored the effect of varying the dimensionless parameter γ in some detail. For large values of γ the quantum pressure term dominates and the wave-mechanical density field is oscillatory as in the time-independent example considered earlier. If the value of γ is chosen to be smaller (e.g. $\gamma = 0.1$), then we find that the quantum pressure is dominant at early times and inhibits the gravitational collapse of the initial density perturbation. However, the exponentially

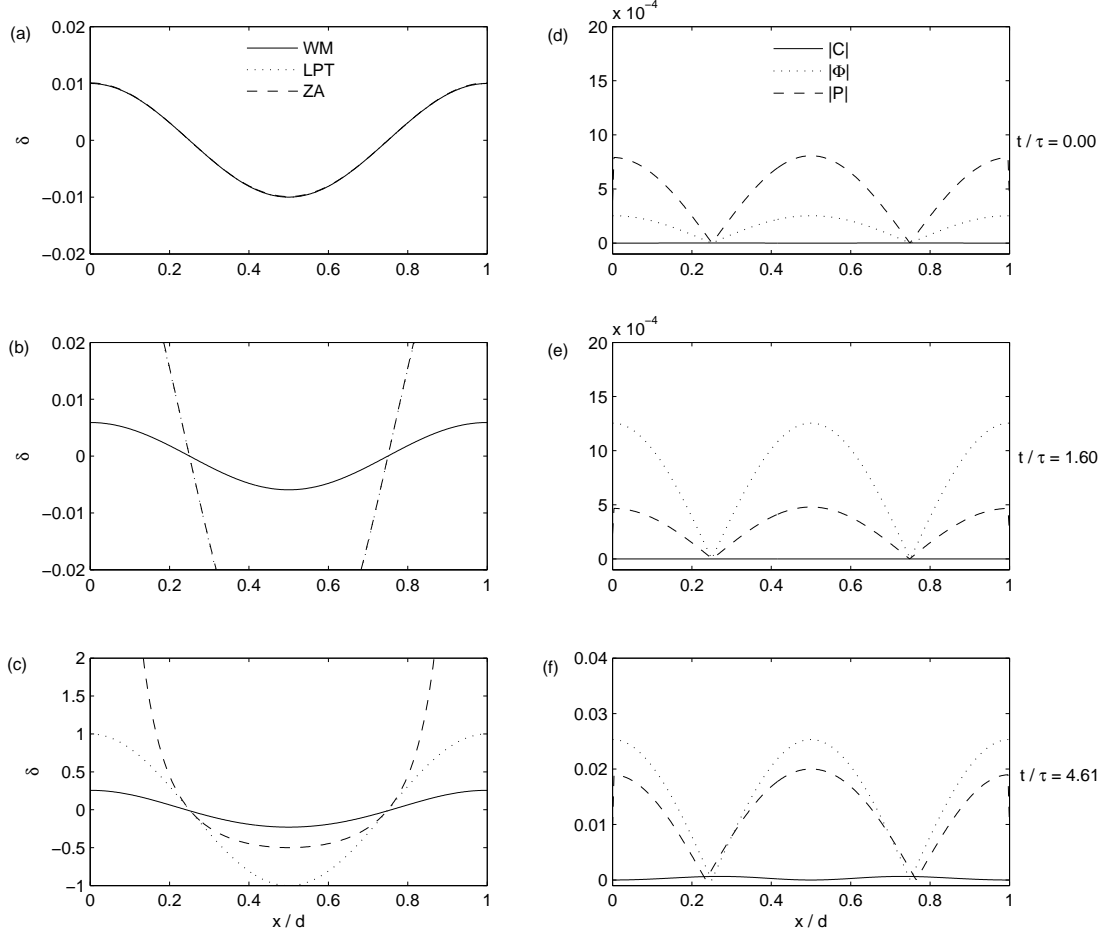


Figure 7. Time-evolution of an initially sinusoidal density perturbation in a static universe. The left-hand plots are as in figure 5, except that the parameter $\gamma = 0.1$ in the wave-mechanical approximation. The right-hand plots show the corresponding evolution of the magnitudes of the convective (C), gravitational potential (Φ) and quantum pressure (P) terms, in units of d^2/τ^2 .

increasing gravitational potential grows rapidly and soon becomes the dominant term in the Bernoulli equation (84). The over-dense regions in the wave-mechanical density field then begin to grow in the usual manner. *A priori* we anticipate that the unwanted effects of the quantum pressure term will be negligible in the limit $\gamma \rightarrow 0$ and so the wave-mechanical approach will yield better results. However, the nature of our perturbative solution of the Schrödinger equation again prevents us from choosing arbitrarily small values of γ . As the value of γ is decreased we find that the perturbative solution of the Schrödinger equation breaks down at progressively earlier times. The onset of non-perturbative behaviour results in the formation of an unphysical over-density at $x = d/2$ in the wave-mechanical density field. For very small values of $\gamma \ll 0.015$ this over-density appears at times very close to the initial time.

Is clear from the above discussion that again we must be very careful in our choice of γ . We find that the optimal value of γ in the case at hand is $\gamma = 0.02$ (figure 6). For this value of γ the quantum pressure is small enough not to prevent the growth of over-densities. At the same time γ is large enough that our second-order perturbative solution of the Schrödinger equation remains valid up until the time of shell-crossing; there is no over-density formed where the gravitational potential is at a maximum.

To summarize, the general properties of our perturbative wave-mechanical approach are found to be the same in both the time-independent and time-dependent gravitational potential cases. However, the wave-mechanical approximation performs significantly better when the potential is allowed to evolve with time, as long as γ is chosen suitably. We find that the wave-mechanical approach agrees well with both LPT and the Zeldovich approximation for times up to $t \approx 2t_{sc}/3$. As the time of shell-crossing approaches, the Zeldovich approximation leads to the formation of large over-densities. The wave-mechanical approximation does not match the Zeldovich approximation in the vicinity of these over-densities, but it does seem to perform better than LPT in such regions. Also, the wave-mechanical and Zeldovich approximation density fields agree in under-dense regions and, unlike the linearized fluid approach, the wave-mechanical approximation does not generate regions with $\delta < -1$ at shell-crossing.

4.2. One-dimensional collapse in an expanding universe

We end our discussion by describing the results obtained from applying the wave-mechanical approach to the study of gravitational collapse in an expanding spatially-flat CDM-dominated universe. Recall that, in this case, the Schrödinger equation to be solved was simply the free-particle Schrödinger equation. This equation is exactly solvable; the solution is given by (68). Upon introducing the dimensionless comoving coordinate $\bar{x} = x/d$ we find that the free-particle solution depends on one dimensionless parameter: $\Gamma = \nu/d^2$. Note that $\Gamma \propto \nu$ and so hereafter we will analyse the behaviour of the wave-mechanical approach in terms of Γ instead.

In the wave-mechanical approximation, the CDM density field is determined from the wavefunction as follows:

$$\delta = |\psi^2| - 1. \quad (91)$$

To calculate the corresponding LPT and Zeldovich approximation density fields we use

$$\delta = \left(\frac{a}{a_i} \right) \delta_i \quad (92)$$

and

$$\delta = \left[1 - \left(\frac{a}{a_i} \right) \delta_i \right]^{-1} - 1, \quad (93)$$

respectively. We set the initial value of the scale factor to $a_i = 0.02$ (which corresponds to an initial redshift $1 + z_i = 50$). Shell-crossing then occurs at $a_{sc} = a_i/\delta_a = 2$ for

$\delta_a = 0.01$. We now use the free-particle version of the wave-mechanical approximation to follow the gravitational evolution of the initial density fluctuation (72) from a_i to a_{sc} . As in the other examples, we will investigate the effect of varying the parameter Γ .

In the previous section we used the wave-mechanical approach to study gravitational collapse in a static universe. We considered two cases: a time-independent and a time-dependent gravitational potential. In both of these situations we were forced to resort to finding approximate solutions of the appropriate Schrödinger equation. To do this we employed perturbation theory. The nature of our perturbative solutions to the Schrödinger equation meant that we were prevented from choosing the dimensionless parameter γ to be arbitrarily small. One might think this problem would be avoided in the present case since the free-particle Schrödinger equation has an exact solution and perturbative solutions are not necessary. However, in practice, there is a lower bound Γ_c on the value of Γ which is of purely numerical origin and arises from the fact that we test the wave-mechanical approach on a (one-dimensional) discrete grid. Sampling at the Nyquist rate (the minimum possible sampling rate) requires that the phase change between two neighbouring grid points must be less than or equal to π radians. The phase of the initial wavefunction is proportional to $1/\Gamma$ and so, in the limit $\Gamma \rightarrow 0$, the phase varies increasingly rapidly and the change in phase between two neighbouring grid points can exceed π radians. The phase is then insufficiently sampled and aliasing effects cause the wave-mechanical approximation to break down. To avoid this problem we must choose $\Gamma \geq \Gamma_c$. In the particular examples presented in this section we have $\Gamma_c = 6 \times 10^{-5}$; the value of Γ_c is found by applying a simple numerical algorithm.

As a general point to note, there is of course an analogous lower bound γ_c on the value of γ in the two examples discussed in the previous section. However, in both cases the perturbative solutions of the Schrödinger equation break down at values of $\gamma > \gamma_c$ and so we do not need to worry about phase-aliasing issues in these particular cases.

The left-hand column of figure 8 shows the wave-mechanical evolution of the initial density perturbation for $\Gamma = \Gamma_c = 6 \times 10^{-5}$. The linearized fluid and Zeldovich approximation density fields are also shown. At $a \approx a_{sc}/3$ the wave-mechanical density field provides a close match to the density fields of the other two approximations. The wave-mechanical approach also agrees well with the Zeldovich approximation (which is exact in one-dimension) at $a \approx 2a_{sc}/3$. This is particularly true in under-dense regions and in the vicinity of the peaks of the density field. As in the Zeldovich approximation large over-densities are formed in the wave-mechanical density field near shell-crossing $a \approx a_{sc}$. However, unlike the Zeldovich approximation, the wave-mechanical approach leads to a density field that remains well behaved at shell-crossing; no singularities are generated.

It is also informative to examine the behaviour of the quantum pressure term in the $\Gamma = 6 \times 10^{-5}$ case. In our wave-mechanical formalism in an expanding universe the quantum pressure term

$$\mathcal{P} = \frac{\nu^2}{2} \frac{\nabla_x^2 \sqrt{(1 + \delta)}}{\sqrt{(1 + \delta)}} \quad (94)$$

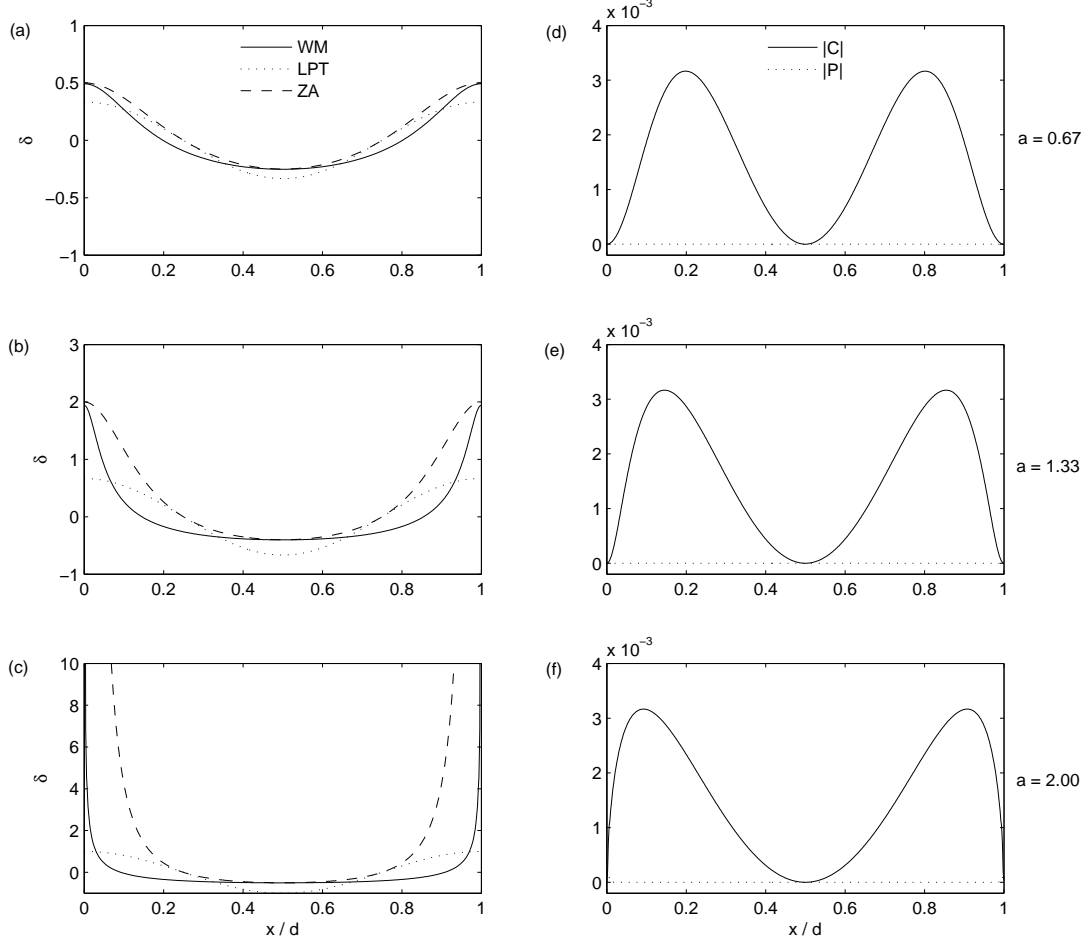


Figure 8. Time-evolution of an initially sinusoidal density perturbation in an expanding spatially-flat CDM-dominated universe. The amplitude of the initial density perturbation is $\delta_a = 0.01$. The left-hand plots show the density fields obtained from the free-particle wave-mechanical approach (WM), the linearized fluid approach (LPT) and the Zeldovich approximation (ZA) at three different values of the scale factor. The parameter $\Gamma = 6 \times 10^{-5}$ in the wave-mechanical approximation. The right-hand plots show the corresponding evolution of the magnitudes of the convective (C) and quantum pressure (P) terms, in units of d^2 .

appears in the modified Bernoulli equation

$$\frac{\partial \phi}{\partial a} + \mathcal{C} + \mathcal{P} = 0, \quad (95)$$

where $\mathcal{C} = \mathcal{C}(x, a)$ is the convective term:

$$\mathcal{C} = -\frac{1}{2} \left(\frac{\partial \phi}{\partial x} \right)^2. \quad (96)$$

Remember that we have set the potential term \mathcal{V} usually appearing in the Bernoulli equation to zero, as it is in the linear and quasi-linear regimes. The right-hand column

of figure 8 compares $|\mathcal{C}|$ and $|\mathcal{P}|$ as functions of the scale factor. We can immediately see that the convective term completely dominates the quantum pressure term at all values of the scale factor and the quantum pressure is negligible.

For completeness we also investigate the behaviour of the wave-mechanical approximation when the value of Γ is increased. We consider the case of $\Gamma = 0.07$ in figure 9. The left-hand column shows how the wave-mechanical density field varies with the scale factor in this case. Figure 9(a) and figure 9(b) show that the wave-mechanical density field evolves as expected up to $a = a_{\text{sc}}/2$; the initially over-dense regions become more dense. However, for $a > a_{\text{sc}}/2$, the over-densities in the wave-mechanical density field cease to grow and begin to decay in the manner seen in the last section. Consequently, at $a = a_{\text{sc}}$, the wave-mechanical density field is not in good agreement with the density fields of LPT and the Zeldovich approximation. We can understand this by inspecting the relative contributions of the quantum pressure and convective terms to the Bernoulli equation (95). The right-hand column of figure 9 shows how the magnitudes of these two terms evolve with the scale-factor. It is clear that the convective term initially dominates the quantum pressure term. However, as the scale factor increases the quantum pressure quickly grows until, at $a = a_{\text{sc}}/2$, it is much larger than the convective term. The large quantum pressure acts to halt the growth of over-densities in the wave-mechanical approximation in some way.

We have seen that the convective term is initially larger than the quantum pressure term for $\Gamma = 0.07$. When the value of $\Gamma \sim 1$, this is no longer true; in such cases the quantum pressure term is the dominant term in Bernoulli equation (95) at all values of the scale-factor up to $a = a_{\text{sc}}$. As in the examples studied in the previous section, the wave-mechanical density field then oscillates rapidly about $\langle \delta \rangle = 0$ (as illustrated in figure 4) and there is no overall growth of the initial density fluctuation.

In this section we have used the wave-mechanical approach to model the gravitational collapse of an initially sinusoidal density perturbation in an expanding spatially-flat CDM-dominated universe. We have found that the dimensionless parameter Γ governs the performance of the wave-mechanical approximation as it controls the quantum pressure term. For large values of Γ , the quantum pressure dominates the convective term and the growth of density perturbations is impeded in the wave-mechanical approach. By reducing Γ we find that the quantum pressure term becomes less influential and the performance of the wave-mechanical approach correspondingly improves. We are especially interested in the limit $\Gamma \rightarrow 0$ as we expect our modified fluid equations to approach the usual classical fluid equations in this limit. Since the solution to the free-particle Schrödinger equation is exact then we do not have to worry about issues surrounding the use of perturbative solutions of the Schrödinger equation in the limit $\Gamma \rightarrow 0$. We find that we are free to reduce the value of Γ until we reach the limit $\Gamma_c = 6 \times 10^{-5}$ imposed by the Nyquist frequency of the discrete grid that we use to test the wave-mechanical approach. For this value of Γ the wave-mechanical approximation performs well in comparison to the linearized fluid approach and the Zeldovich approximation; see figure 8.

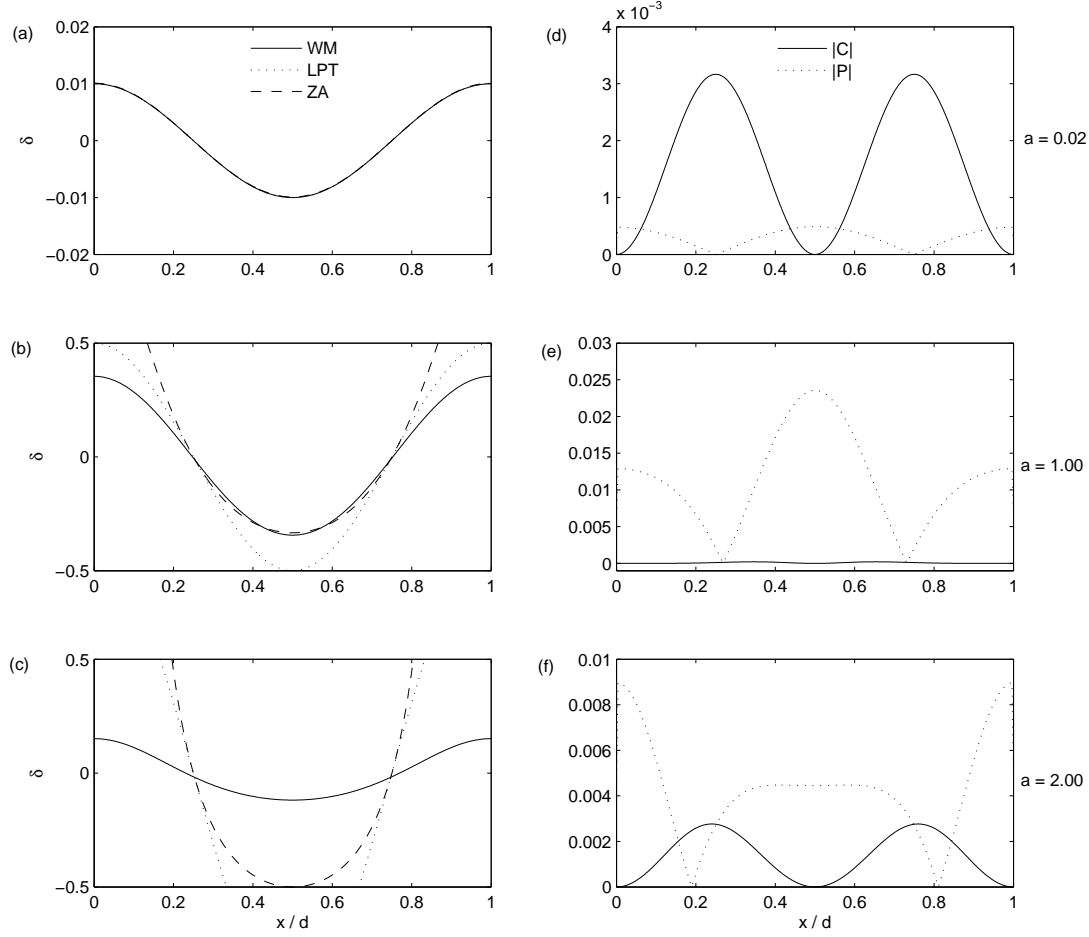


Figure 9. Time-evolution of an initially sinusoidal density perturbation in an expanding universe. The layout of the plots is as in figure 8; the only difference is that the parameter $\Gamma = 0.07$ in the wave-mechanical approximation.

5. Conclusion

In this paper we have studied in some detail the behaviour of the wave-mechanical approach in simple gravitational collapse scenarios. We have used the Schrödinger equation to model the evolution of a one-dimensional sinusoidal density perturbation in the CDM distribution in both static and expanding universes. The aim of considering such simple examples was to elucidate the effect of varying the free parameter ν (or, equivalently, γ and Γ) in the wave-mechanical formalism.

As a first step we assumed a static background dominated by CDM with a cosmological constant. We considered two distinct situations: a time-independent and a time-dependent gravitational potential. In both of these cases, the resulting Schrödinger equation was not exactly solvable and so we employed standard quantum-mechanical

approximation methods to calculate solutions of the Schrödinger equation.

An approximate solution of the Schrödinger equation with a time-independent potential was found by applying first-order time-independent perturbation theory. In this case, the wave-mechanical approach performed relatively poorly in comparison with the established linearized fluid approach and the Zeldovich approximation. However, the assumption of a fixed gravitational potential is not physically realistic as it is not a consistent solution of the linearized equations of motion. Nevertheless, this simple example did illustrate most effectively some of the salient qualitative aspects of the behaviour of the system in general. We have seen that for large values of ν , the quantum pressure becomes important and acts to impede the collapse of density perturbations in some way. This suggests that we should choose the value of ν to be as small as possible in order to minimize the effect of the quantum pressure term. Remember that it is in this limit that our hydrodynamical description of quantum mechanics should approach the usual classical hydrodynamical equations. However, our perturbative solution of the Schrödinger equation breaks down as the value of ν is reduced and so we cannot choose the value of ν to be arbitrarily small. In order for our perturbative wave-mechanical approach to yield sensible results, we must be extremely careful in choosing the value of ν .

The performance of the wave-mechanical approximation improved considerably when we allowed the gravitational potential appearing in the Schrödinger equation to evolve with time. In this case, we used second-order time-dependent perturbation theory to determine an approximate solution of the Schrödinger equation. Again, the perturbative nature of our solution prevented us from choosing arbitrarily small values of ν . However, it was possible to choose a value of ν such that the quantum pressure was small enough not to inhibit the growth of over-densities and yet the perturbation expansion of the wavefunction remained stable. For this choice of ν , we found that the wave-mechanical approach compared favourably with LPT and the Zeldovich approximation.

The behaviour of these two examples for different values of ν perhaps yield the most important insights of this paper. In general cosmological models, we do not expect the Schrödinger-Poisson system to be exactly solvable and so one must resort to either finding numerical or approximate solutions. As we have said, we are especially interested in solutions of this system in the limit $\nu \rightarrow 0$ where the quantum pressure is expected to be negligibly small. However, by studying simple examples, we have demonstrated that there are issues regarding the construction of perturbative solutions of the Schrödinger equation in this limit. This promises to be useful in future work.

We have also used the wave-mechanical approach to study gravitational collapse in the more physically relevant case of an expanding, spatially-flat universe dominated by CDM. In this special case, we have seen that the Schrödinger equation can be conveniently reduced to the free-particle Schrödinger equation. The solution of this equation is exact rather than perturbative and, consequently, the problems encountered in the other examples at small ν do not apply. However, there is still a lower bound ν_c on

the value of ν which arises from the fact that we test the wave-mechanical approximation on a discrete grid. For $\nu = \nu_c$ we find that the quantum pressure term is indeed negligibly small and the free-particle wave-mechanical approximation performs well in comparison with LPT and the Zeldovich approximation. Large over-densities are generated in the wave-mechanical density field as in the Zeldovich approximation. However, the wave-mechanical approach behaves much more smoothly than the Zeldovich approximation at times close to shell-crossing; no singularities are formed in the density field at shell-crossing and so the method does not fail catastrophically when caustics are formed. The success of this free-particle formulation of the wave-mechanical approach in the simple example presented here suggests that this method promises to be a useful tool for modelling the formation of large-scale structure in the universe. This idea is explored in detail elsewhere (Short and Coles 2006).

Finally, another attractive property of the wave-mechanical approximation is that the matter density field remains positive at all times, even after shell-crossing has occurred. This fact, along with the unitary structure of quantum mechanics, suggests that the wave-mechanical approach could be applied to the problem of cosmological reconstruction.

Acknowledgments

C J Short would like to thank PPARC for the award of a studentship that made this work possible.

Appendix A. Perturbative solutions of the one-dimensional Schrödinger equation

In section 3.1 of this paper we used the wave-mechanical approach to study the gravitational evolution of a one-dimensional sinusoidal density perturbation in a static universe. The appropriate Schrödinger equation to be solved was of the form

$$i\nu \frac{\partial \psi}{\partial t} = \left[-\frac{\nu^2}{2} \frac{\partial^2}{\partial x^2} + \Phi \right] \psi, \quad (\text{A.1})$$

where the gravitational potential Φ was initially chosen to be time-independent (section 3.1.1):

$$\Phi = -\delta_a \left(\frac{d}{2\pi\tau} \right)^2 \cos \left(\frac{2\pi x}{d} \right), \quad (\text{A.2})$$

and then allowed to evolve with time (section 3.1.2):

$$\Phi = -\delta_a \left(\frac{d}{2\pi\tau} \right)^2 \exp \left(\frac{t - t_i}{\tau} \right) \cos \left(\frac{2\pi x}{d} \right). \quad (\text{A.3})$$

The Schrödinger equation (A.1) is written in the position representation. It can be written in a more general form without referring to a particular basis as

$$i\nu \frac{d}{dt} |\psi(t)\rangle = \hat{H} |\psi(t)\rangle, \quad (\text{A.4})$$

where $|\psi(t)\rangle$ is a general ket representing the state of the physical system at time t and \hat{H} is the total Hamiltonian. The state ket $|\psi(t)\rangle$ is related to the initial state ket $|\psi_i\rangle = |\psi(t_i)\rangle$ by

$$|\psi(t)\rangle = \hat{U}(t, t_i) |\psi_i\rangle, \quad (\text{A.5})$$

where $\hat{U}(t, t_i)$ is the unitary time-evolution operator. Substituting (A.5) into the general Schrödinger equation (A.4) yields the following equation for the time-evolution operator:

$$i\nu \frac{d}{dt} \hat{U}(t, t_i) = \hat{H} \hat{U}(t, t_i). \quad (\text{A.6})$$

In the case of a time-independent potential, the total Hamiltonian \hat{H} does not depend on time and can be written as $\hat{H} = \hat{H}_0 + \hat{\Phi}$ where $\hat{H}_0 = \hat{P}^2/2$ is the free-particle Hamiltonian (with \hat{P} the momentum operator) and $\hat{\Phi}$ is the potential (A.2) in operator form. If, on the other hand, the potential depends on time then the Hamiltonian also depends explicitly on time and we write $\hat{H} = \hat{H}(t)$ to signify this. The Hamiltonian $\hat{H}(t)$ can be split in a similar fashion: $\hat{H}(t) = \hat{H}_0 + \hat{\Phi}(t)$ where $\hat{\Phi}(t)$ is the time-dependent potential (A.3) in operator form. In both cases the Schrödinger equation (A.4) cannot be solved exactly. However, we can view the potential as a perturbation to the free-particle Hamiltonian and so this suggests that we can construct approximate solutions to (A.4) using time-independent and time-dependent perturbation theory, respectively. Before continuing we first describe how to solve the free-particle Schrödinger equation

$$i\nu \frac{d}{dt} |\psi(t)\rangle = \hat{H}_0 |\psi(t)\rangle, \quad (\text{A.7})$$

as this will be of use when developing perturbative solutions of (A.4).

Appendix A.1. The free-particle Schrödinger equation

The free-particle Hamiltonian \hat{H}_0 is independent of time and so, upon substituting (A.5) into (A.7) and integrating, we find that

$$\hat{U}(t, t_i) = \exp \left[\frac{-i(t - t_i)\hat{H}_0}{\nu} \right]. \quad (\text{A.8})$$

In order to evaluate the effect of the time-evolution operator (A.8) on a general initial ket $|\psi_i\rangle$, we must know how it acts on the base kets used in expanding $|\psi_i\rangle$. The initial state ket can be expanded in terms of orthonormal energy eigenkets $|n^{(0)}\rangle$ of \hat{H}_0 as

$$|\psi_i\rangle = \sum_n a_n |n^{(0)}\rangle, \quad (\text{A.9})$$

where $a_n = \langle n^{(0)} | \psi_i \rangle$ and the energy eigenkets $|n^{(0)}\rangle$ satisfy the general time-independent free-particle Schrödinger equation

$$\hat{H}_0 |n^{(0)}\rangle = E_n^{(0)} |n^{(0)}\rangle. \quad (\text{A.10})$$

The state ket at time t is then found by substituting the time-evolution operator (A.8) and the initial ket expansion (A.9) into (A.5) giving

$$|\psi(t)\rangle = \sum_n a_n \exp \left[\frac{-i(t-t_i)E_n^{(0)}}{\nu} \right] |n^{(0)}\rangle. \quad (\text{A.11})$$

Thus the any initial-value problem can be completely solved once the energy eigenvalues $E_n^{(0)}$ and eigenkets $|n^{(0)}\rangle$ of $\hat{H}^{(0)}$ are known, i.e. once the eigenvalue problem (A.10) has been solved. In order to solve (A.10) it is convenient to rewrite it in the position representation:

$$-\frac{\nu^2}{2} \frac{d^2 \phi_n^{(0)}}{dx^2} = E_n^{(0)} \phi_n^{(0)}, \quad (\text{A.12})$$

where $\phi_n^{(0)} = \phi_n^{(0)}(x)$ are the energy eigenfunctions, defined by $\phi_n^{(0)} = \langle x | n^{(0)} \rangle$. Upon introducing $k_n^2 = 2E_n^{(0)}/\nu^2$ (A.12) becomes

$$\left(\frac{d^2}{dx^2} + k_n^2 \right) \phi_n^{(0)} = 0, \quad (\text{A.13})$$

and the solutions to this equation are of the form

$$\phi_n^{(0)} = \frac{1}{L^{3/2}} \exp(ik_n x). \quad (\text{A.14})$$

As before we are considering a cubic volume of side length L equipped with periodic boundary conditions at each face. The allowed values of the wavenumber k_n then form a discrete spectrum: $k_n = 2n\pi/L$, n an integer. The pre-factor $1/L^{3/2}$ comes from the requirement that the energy eigenfunctions are normalized.

The time-independent free-particle Schrödinger equation has now been completely solved in the sense that all energy eigenvalues $E_n^{(0)} = \nu^2 k_n^2/2$ and energy eigenfunctions $\phi_n^{(0)}$ are known and the set $\{\phi_n^{(0)}\}$ is orthonormal. To complete the solution (A.11) of the free-particle Schrödinger equation we need to determine the coefficients a_n .

Appendix A.1.1. Calculating the expansion coefficients The expansion coefficients $a_n = \langle n^{(0)} | \psi_i \rangle$ can be found from

$$a_n = L^2 \int_0^L \overline{\phi_n^{(0)}}(x) \psi_i(x) dx, \quad (\text{A.15})$$

where $\psi_i = \langle x | \psi_i \rangle$ and an overline denotes complex conjugation. We again divide the cubic volume into cells of side length d , i.e. set $L = Nd$, $N > 0$ an integer. We can then write (A.15) as

$$a_n = L^2 \sum_{j=0}^{N-1} \int_{jd}^{(j+1)d} \overline{\phi_n^{(0)}}(x) \psi_i(x) dx \quad (\text{A.16})$$

Performing a change of variable $x' = x - jd$ leads to

$$a_n = L^2 \sum_{j=0}^{N-1} \int_0^d \overline{\phi_n^{(0)}}(x' + jd) \psi_i(x' + jd) dx' \quad (\text{A.17})$$

It is clear from (A.14) that the eigenfunctions $\phi_n^{(0)}$ satisfy the condition

$$\phi_n^{(0)}(x \pm jd) = \exp(\pm ijk_nd) \phi_n^{(0)}(x), \quad (\text{A.18})$$

where $k_nd = 2n\pi/N$ and j is an integer. This condition is known as Bloch's theorem (Bloch 1928) which holds for energy eigenfunctions of any periodic Hamiltonian.

The initial density field δ_i we are considering is periodic with period d . Consequently the initial velocity potential φ_i is also periodic with the same period. It follows that the initial wavefunction $\psi_i = \sqrt{\rho_i} \exp(-i\varphi_i/\nu)$ also has a period of d , i.e. $\psi_i(x+jd) = \psi_i(x)$. Using this fact along with (A.18) in (A.17) yields

$$a_n = L^2 \int_0^d \overline{\phi_n^{(0)}}(x') \psi_i(x') dx' \sum_{j=0}^{N-1} \exp(-ijk_nd). \quad (\text{A.19})$$

A significant simplification can be made by noting that

$$\sum_{j=0}^{N-1} \exp(-ijk_nd) = N\delta_{n,pN}, \quad (\text{A.20})$$

where p is an integer. In other words, the coefficients a_n are zero unless n is an integer multiple of N :

$$a_n = NL^2 \delta_{n,pN} \int_0^d \overline{\phi_n^{(0)}}(x') \psi_i(x') dx'. \quad (\text{A.21})$$

It is immediately clear from (A.14) that the expansion coefficients are simply found by taking the Fourier transform of the initial wavefunction.

The full solution to the free-particle Schrödinger equation (A.7) then appears in the position representation as

$$\psi = \sum_n a_n \exp\left[\frac{-i(t - t_i)E_n^{(0)}}{\nu}\right] \phi_n^{(0)}, \quad (\text{A.22})$$

with $\psi = \langle x | \psi(t) \rangle$.

Appendix A.2. The Schrödinger equation with a time-independent external potential

We now turn our attention to solving the Schrödinger equation (A.4) with a time-independent Hamiltonian of the form $\hat{H} = \hat{H}_0 + \hat{\Phi}$ where the potential is given by (A.2) in the position representation. Since the Hamiltonian does not depend on time then, as in the free-particle case, the solution of (A.4) will be of the form

$$|\psi(t)\rangle = \sum_n b_n \exp\left[\frac{-i(t - t_i)E_n}{\nu}\right] |n\rangle, \quad (\text{A.23})$$

where $b_n = \langle n | \psi_i \rangle$. The energy eigenvalues E_n and eigenkets $|n\rangle$ are solutions of the time-independent Schrödinger equation (TISE)

$$\hat{H} |n\rangle = E_n |n\rangle. \quad (\text{A.24})$$

The expansion coefficients $b_n = \langle n | \psi_i \rangle$ can be determined from

$$b_n = L^2 \int_0^L \overline{\phi_n}(x) \psi_i(x) dx, \quad (\text{A.25})$$

where $\phi_n = \langle x | n \rangle$ are the energy eigenfunctions of the total Hamiltonian. Since the Hamiltonian is periodic with period d then the eigenfunctions must satisfy Bloch's theorem. We can then perform an analogous calculation to the one presented in Appendix A.1.1 to find

$$b_n = NL^2 \delta_{n,pN} \int_0^d \overline{\phi_n}(x) \psi_i(x) dx, \quad (\text{A.26})$$

and so, as before, the expansion coefficients b_n are zero unless n is an integer multiple of N . This result will prove helpful later.

Now that we have derived an expression for the expansion coefficients, the solution (A.23) to the Schrödinger equation will be complete once we have found the energy eigenvalues E_n and eigenkets $|n\rangle$ of the TISE (A.24). For the particular potential we are considering, the TISE is in fact an instance of *Mathieu's equation*. This equation is exactly solvable; however, in this paper we are interested in perturbative solutions of the Schrödinger equation and so we appeal to first order time-independent perturbation theory to construct an approximate solution instead.

Appendix A.2.1. Time-independent perturbation theory To perturbatively solve (A.24) we rewrite the perturbing potential $\hat{\Phi}$ as $\lambda \hat{\Phi}$ where $\lambda \in [0, 1]$. The TISE then becomes

$$(\hat{H}_0 + \lambda \hat{\Phi}) |n\rangle = E_n |n\rangle. \quad (\text{A.27})$$

In the limit $\lambda \rightarrow 0$ the previously solved time-independent free-particle Schrödinger equation (A.10) is recovered. As λ is increased from zero (i.e. as the perturbation is 'switched on'), we expect the energy eigenvalue E_n to depart from its unperturbed value $E_n^{(0)}$ and so we define the energy shift Δ_n for the n th level as

$$\Delta_n \equiv E_n - E_n^{(0)}. \quad (\text{A.28})$$

The TISE (A.27) can then be written in the form

$$(E_n^{(0)} - \hat{H}_0) |n\rangle = (\lambda \hat{\Phi} - \Delta_n) |n\rangle. \quad (\text{A.29})$$

We would like to invert the operator $(E_n^{(0)} - \hat{H}_0)$. However, the inverse operator $(E_n^{(0)} - \hat{H}_0)^{-1}$ is ill defined since it may act on $|n^{(0)}\rangle$ and $(E_n^{(0)} - \hat{H}_0)^{-1} |n^{(0)}\rangle$ is undefined. Define the complementary projection operator φ_n by

$$\begin{aligned}\varphi_n &\equiv 1 - |n^{(0)}\rangle \langle n^{(0)}| \\ &= \sum_{j \neq n} |j^{(0)}\rangle \langle j^{(0)}|,\end{aligned}\tag{A.30}$$

then the inverse operator $(E_n^{(0)} - \hat{H}_0)^{-1}$ is well defined when it acts on φ_n from the left:

$$\frac{1}{E_n^{(0)} - \hat{H}_0} \varphi_n = \sum_{j \neq n} \frac{1}{E_n^{(0)} - E_j^{(0)}} |j^{(0)}\rangle \langle j^{(0)}|.\tag{A.31}$$

Note that (A.29) implies $\langle n^{(0)} | (\lambda \hat{\Phi} - \Delta_n) | n \rangle = 0$. Using (A.30) it is then evident that

$$(\lambda \hat{\Phi} - \Delta_n) |n\rangle = \varphi_n (\lambda \hat{\Phi} - \Delta_n) |n\rangle,\tag{A.32}$$

and so the TISE (A.29) can be written as

$$|n\rangle = c_n(\lambda) |n^{(0)}\rangle + \frac{1}{E_n^{(0)} - \hat{H}_0} \varphi_n (\lambda \hat{\Phi} - \Delta_n) |n\rangle,\tag{A.33}$$

where $c_n(\lambda) \rightarrow 1$ as $\lambda \rightarrow 0$ and the term $c_n(\lambda) |n^{(0)}\rangle$ ensures that in the limit $\lambda \rightarrow 0$ we have $|n\rangle \rightarrow |n^{(0)}\rangle$. It is convenient to depart from the usual normalization convention $\langle n | n \rangle = 1$ and set $\langle n^{(0)} | n \rangle = c_n(\lambda) = 1$. Then, using $\langle n^{(0)} | (\lambda \hat{\Phi} - \Delta_n) | n \rangle = 0$, we find that

$$\Delta_n = \lambda \langle n^{(0)} | \hat{\Phi} | n \rangle.\tag{A.34}$$

The two fundamental equations are (A.33) and (A.34). The basic strategy is to expand $|n\rangle$ and Δ_n in powers of λ as follows:

$$|n\rangle = |n^{(0)}\rangle + \lambda |n^{(1)}\rangle + \lambda^2 |n^{(2)}\rangle + \dots,\tag{A.35}$$

$$\Delta_n = \lambda \Delta_n^{(1)} + \lambda^2 \Delta_n^{(2)} + \dots.\tag{A.36}$$

Substituting (A.35) and (A.36) into (A.33) and (A.34) and equating terms of $\mathcal{O}(\lambda)$ we obtain

$$|n^{(1)}\rangle = \frac{1}{E_n^{(0)} - \hat{H}_0} \varphi_n \hat{\Phi} |n^{(0)}\rangle,\tag{A.37}$$

$$\Delta_n^{(1)} = \langle n^{(0)} | \hat{\Phi} | n^{(0)} \rangle.\tag{A.38}$$

The expression (A.31) can be used to write (A.37) as

$$|n^{(1)}\rangle = \sum_{j \neq n} \frac{1}{E_n^{(0)} - E_j^{(0)}} |j^{(0)}\rangle \langle j^{(0)} | \hat{\Phi} | n^{(0)} \rangle,\tag{A.39}$$

where the matrix elements $\langle j^{(0)} | \hat{\Phi} | n^{(0)} \rangle$ are given by

$$\langle j^{(0)} | \hat{\Phi} | n^{(0)} \rangle = L^2 \int_0^L \overline{\phi_j^{(0)}(x)} \Phi(x) \phi_n^{(0)}(x) dx.\tag{A.40}$$

Substituting Φ from (A.2) and remembering that $L = Nd$ then yields

$$\langle j^{(0)} | \hat{\Phi} | n^{(0)} \rangle = -\frac{\delta_a}{2} \left(\frac{d}{2\pi\tau} \right)^2 \sum_{s=\pm 1} \delta_{j,n+sN}, \quad (\text{A.41})$$

and so, using $E_n^{(0)} = \nu^2 k_n^2 / 2$, we obtain

$$|n^{(1)}\rangle = \frac{\delta_a}{16\pi^3\gamma^2} \sum_{s=\pm 1} \frac{1}{s(k_n d + s\pi)} |n + sN^{(0)}\rangle, \quad (\text{A.42})$$

where $k_n d = 2n\pi/N$ and $\gamma = \nu\tau/d^2$ is a dimensionless parameter. Correspondingly, inserting the matrix elements (A.41) into the equation (A.38) for the first order energy shift $\Delta_n^{(1)}$ yields

$$\Delta_n^{(1)} = 0. \quad (\text{A.43})$$

In summary, to first order, the perturbed eigenkets and energy eigenvalues are given by

$$|n\rangle = |n^{(0)}\rangle + \lambda \frac{\delta_a}{16\pi^3\gamma^2} \sum_{s=\pm 1} \frac{1}{s(k_n d + s\pi)} |n + sN^{(0)}\rangle, \quad (\text{A.44})$$

$$E_n = \frac{\nu^2 k_n^2}{2}, \quad (\text{A.45})$$

respectively. It is immediately clear from the first order expression (A.44) for the perturbed eigenket $|n\rangle$ that at the band edges $k_n d = \pm\pi$ (i.e. $n = \pm N/2$) the coefficients of the perturbation expansion become singular and the series no longer converges. This problem is due to a degeneracy and so it seems as if we will have to perform a lengthy time-independent degenerate perturbation theory calculation to determine the kets $|\pm N/2\rangle$. However, this can be avoided by remembering that the expansion coefficients b_n appearing in the solution (A.23) of the Schrödinger equation (A.4) are zero unless n is an integer multiple of N . This implies that the coefficients $b_{\pm N/2} = 0$ and so we do not need to calculate the kets $|\pm N/2\rangle$ anyway.

The final step is to normalize the eigenkets. Recall that we used the normalization condition $\langle n^{(0)} | n \rangle = 1$ to derive the perturbed ket (A.44) and so the ket $|n\rangle$ is not normalized in the usual manner. The perturbed ket can be renormalized by defining

$$|n\rangle^\dagger \equiv Z_n^{1/2} |n\rangle, \quad (\text{A.46})$$

where Z_n is a constant chosen so that ${}^\dagger \langle n | n \rangle^\dagger = 1$. Noting that ${}^\dagger \langle n | n \rangle^\dagger = Z_n \langle n | n \rangle$ then, for the ket $|n\rangle^\dagger$ to be normalized, we must have

$$\begin{aligned} Z_n^{-1} &= \langle n | n \rangle \\ &= (\langle n^{(0)} | + \lambda \langle n^{(1)} | + \dots) (\langle n^{(0)} | + \lambda \langle n^{(1)} | + \dots) \\ &= 1 + \lambda^2 \langle n^{(1)} | n^{(1)} \rangle + \dots. \end{aligned} \quad (\text{A.47})$$

Therefore, to $\mathcal{O}(\lambda)$, $Z_n = 1$ and so $|n\rangle^\dagger = |n\rangle$ to first order.

Appendix A.2.2. Summary In the preceding section we used first-order time-independent perturbation theory to find the energy eigenkets $|n\rangle$ and eigenvalues E_n of the TISE (A.24). Recall that the solution to the full Schrödinger equation (A.4) is of the form

$$|\psi(t)\rangle = \sum_n b_n \exp\left[\frac{-i(t-t_i)E_n}{\nu}\right] |n\rangle, \quad (\text{A.48})$$

where the energy eigenvalues are $E_n = \nu^2 k_n^2/2$ with $k_n = 2n\pi/L$ and $L = Nd$. The expansion coefficients b_n are given by (A.26) and are zero unless n is an integer multiple of N . The eigenkets $|n\rangle$ are obtained from (A.44) upon setting $\lambda = 1$. In the position representation (A.48) becomes

$$\psi = \sum_n b_n \exp\left[\frac{-i(t-t_i)E_n}{\nu}\right] \phi_n, \quad (\text{A.49})$$

where the wavefunction $\psi = \psi(x, t)$ and energy eigenfunctions $\phi_n = \phi_n(x)$ are given by $\psi = \langle x|\psi(t)\rangle$ and $\phi_n = \langle x|n\rangle$ respectively. Using (A.44) it follows that the eigenfunctions ϕ_n are of the form

$$\phi_n = \sum_{j=0}^1 \phi_n^{(j)}, \quad (\text{A.50})$$

where $\phi_n^{(0)} = \phi_n^{(0)}(x)$ are the eigenfunctions (A.14) of the time-independent free-particle Schrödinger equation and

$$\phi_n^{(1)} = \frac{\delta_a}{16\pi^3\gamma^2} \phi_n^{(0)} \sum_{s=\pm 1} \frac{1}{s(k_n d + s\pi)} \exp\left(\frac{2is\pi x}{d}\right). \quad (\text{A.51})$$

Appendix A.3. The Schrödinger equation with a time-dependent external potential

In this section we aim to solve the Schrödinger equation (A.4) with a time-dependent Hamiltonian of the form $\hat{H}(t) = \hat{H}_0 + \hat{\Phi}(t)$ where the potential is given by (A.3) in the position representation. To begin with, recall that

$$|\psi(t)\rangle = \hat{U}(t, t_i) |\psi_i\rangle, \quad (\text{A.52})$$

where the time-evolution operator obeys the Schrödinger equation

$$i\nu \frac{d}{dt} \hat{U}(t, t_i) = \hat{H}(t) \hat{U}(t, t_i). \quad (\text{A.53})$$

The previously determined eigenkets $|n^{(0)}\rangle$ of the free-particle Hamiltonian \hat{H}_0 form an orthonormal set and so we may expand the initial state ket $|\psi_i\rangle$ as

$$|\psi_i\rangle = \sum_n a_n |n^{(0)}\rangle, \quad (\text{A.54})$$

where the expansion coefficients $a_n = \langle n^{(0)}|\psi_i\rangle$ are given by (A.21). Once the coefficients are known the initial state ket (A.54) is completely specified. In order to determine the

state ket $|\psi(t)\rangle$ at a time t , it is clear from (A.52) that we require an expression for the time-evolution operator $\hat{U}(t, t_i)$. Since the Hamiltonian now depends explicitly on time, we can no longer simply integrate (A.53) to obtain an expression for the time-evolution operator as we did in the time-independent case. The strategy in such a situation is to seek an approximate expression for the time-evolution operator. We use time-dependent perturbation theory to find a second-order approximate solution of the Schrödinger equation for the time-evolution operator (A.53).

Appendix A.3.1. Time-dependent perturbation theory Before proceeding to perturbatively solve equation (A.53) for the time-evolution operator $\hat{U}(t, t_i)$ it is convenient to introduce another equivalent description of quantum dynamics known as the interaction picture. So far in this work the Schrödinger picture has been used exclusively and all quantities are assumed to be described in this picture unless otherwise specified.

A general state ket in the interaction picture $|\psi(t)\rangle^{(I)}$ is related to the state ket in the Schrödinger picture $|\psi(t)\rangle$ by

$$|\psi(t)\rangle^{(I)} = \hat{U}_0^\dagger(t, t_i) |\psi(t)\rangle, \quad (\text{A.55})$$

where the time-evolution operator $\hat{U}_0(t, t_i)$ is given by

$$\hat{U}_0(t, t_i) = \exp \left[\frac{-i(t - t_i)\hat{H}_0}{\nu} \right], \quad (\text{A.56})$$

and $\hat{U}_0^\dagger(t, t_i)$ denotes the adjoint of $\hat{U}_0(t, t_i)$. The superscript (I) will be used throughout to denote quantities in the interaction picture. Note that $|\psi_i\rangle^{(I)} = |\psi_i\rangle$ and so the interaction and Schrödinger picture state kets coincide at the initial time $t = t_i$.

In the interaction picture a general state ket evolves according to:

$$i\nu \frac{d}{dt} |\psi(t)\rangle^{(I)} = \hat{\Phi}^{(I)}(t) |\psi(t)\rangle^{(I)}, \quad (\text{A.57})$$

where $\hat{\Phi}^{(I)}(t) \equiv \hat{U}_0^\dagger(t, t_i) \hat{\Phi}(t) \hat{U}_0(t, t_i)$ is the perturbing potential in the interaction picture. It is clear from (A.57) that the time evolution of a state ket in the interaction picture is determined solely by $\hat{\Phi}^{(I)}(t)$.

The objective is now to obtain a perturbation expansion for the time-evolution operator $\hat{U}(t, t_i)$ in the Schrödinger picture. This is best achieved by first finding a perturbation expansion for the time-evolution operator in the interaction picture. In this picture a time-evolution operator $\hat{U}^{(I)}(t, t_i)$ can be defined by

$$|\psi(t)\rangle^{(I)} = \hat{U}^{(I)}(t, t_i) |\psi_i\rangle^{(I)}. \quad (\text{A.58})$$

Substituting (A.58) into (A.57) it is clear that $\hat{U}^{(I)}(t, t_i)$ obeys

$$i\nu \frac{d}{dt} \hat{U}^{(I)}(t, t_i) = \hat{\Phi}^{(I)}(t) \hat{U}^{(I)}(t, t_i), \quad (\text{A.59})$$

where this equation must be solved subject to the initial condition $\hat{U}^{(I)}(t_i, t_i) = I$ with I the identity operator. Observe that equation (A.59), together with the appropriate initial condition, is equivalent to the integral equation

$$\hat{U}^{(I)}(t, t_i) = I - \frac{i}{\nu} \int_{t_i}^t \hat{\Phi}^{(I)}(t') \hat{U}^{(I)}(t', t_i) dt'. \quad (\text{A.60})$$

The integral equation (A.60) provides a convenient means of determining a perturbation expansion for $\hat{U}^{(I)}(t, t_i)$. By iteration we find that the time-evolution operator in the interaction picture is given by

$$\hat{U}^{(I)}(t, t_i) = I - \frac{i}{\nu} \int_{t_i}^t dt' \hat{\Phi}^{(I)}(t') - \frac{1}{\nu^2} \int_{t_i}^t dt' \int_{t_i}^{t'} dt'' \hat{\Phi}^{(I)}(t') \hat{\Phi}^{(I)}(t''), \quad (\text{A.61})$$

to second order.

To determine the corresponding time-evolution operator $\hat{U}(t, t_i)$ in the Schrödinger picture, first note that $|\psi(t)\rangle^{(I)} = \hat{U}^{(I)}(t, t_i) |\psi_i\rangle^{(I)} = \hat{U}^{(I)}(t, t_i) |\psi_i\rangle$ since the state kets in the interaction and Schrödinger pictures coincide at $t = t_i$. Using the definition (A.55) it follows that

$$|\psi(t)\rangle = \hat{U}_0(t, t_i) \hat{U}^{(I)}(t, t_i) |\psi_i\rangle. \quad (\text{A.62})$$

Upon comparison with (A.52) it is immediately clear that the time-evolution operator in the Schrödinger picture $\hat{U}(t, t_i)$ is related to $\hat{U}^{(I)}(t, t_i)$ via

$$\hat{U}(t, t_i) = \hat{U}_0(t, t_i) \hat{U}^{(I)}(t, t_i). \quad (\text{A.63})$$

Multiplying (A.61) by $\hat{U}_0(t, t_i)$, inserting $\hat{\Phi}^{(I)}(t) = \hat{U}_0^\dagger(t, t_i) \hat{\Phi}(t) \hat{U}_0(t, t_i)$ and using the following property of the time-evolution operator: $\hat{U}_0(t, t_i) \hat{U}_0^\dagger(t', t_i) = \hat{U}_0(t, t_i) \hat{U}_0(t_i, t') = \hat{U}_0(t, t')$ then gives

$$\hat{U}(t, t_i) = \sum_{j=0}^2 \hat{U}_j(t, t_i), \quad (\text{A.64})$$

to second order, where $\hat{U}_0(t, t_i)$ is given by (A.56),

$$\hat{U}_1(t, t_i) = -\frac{i}{\nu} \int_{t_i}^t dt' \hat{U}_0(t, t') \hat{\Phi}(t') \hat{U}_0(t', t_i), \quad (\text{A.65})$$

and

$$\hat{U}_2(t, t_i) = -\frac{1}{\nu^2} \int_{t_i}^t dt' \int_{t_i}^{t'} dt'' \hat{U}_0(t, t') \hat{\Phi}(t') \hat{U}_0(t', t'') \hat{\Phi}(t'') \hat{U}_0(t'', t_i). \quad (\text{A.66})$$

The second-order expression for the time-evolution operator (A.64) can be inserted into (A.52) along with the initial ket expansion (A.54) to give the following approximate solution to the Schrödinger equation (A.4):

$$|\psi(t)\rangle = \sum_{j=0}^2 |\psi^{(j)}(t)\rangle, \quad (\text{A.67})$$

where

$$|\psi^{(j)}(t)\rangle = \sum_n a_n \hat{U}_j(t, t_i) |n^{(0)}\rangle, \quad (\text{A.68})$$

with $\hat{U}_0(t, t_i)$, $\hat{U}_1(t, t_i)$ and $\hat{U}_2(t, t_i)$ given by (A.56), (A.65) and (A.66), respectively. The zeroth-order state ket $|\psi^{(0)}(t)\rangle$ is then

$$|\psi^{(0)}(t)\rangle = \sum_n a_n \exp \left[\frac{-i(t - t_i) E_n^{(0)}}{\nu} \right] |n^{(0)}\rangle, \quad (\text{A.69})$$

where the energy eigenvalues $E_n^{(0)} = \nu^2 k_n^2 / 2$ and $k_n = 2n\pi/L$. This is simply the solution to the free-particle Schrödinger equation discussed earlier.

The eigenkets $|n^{(0)}\rangle$ of \hat{H}_0 do not depend on time. Using this fact, we find that the state ket $|\psi^{(1)}(t)\rangle$ can be written as

$$|\psi^{(1)}(t)\rangle = -\frac{i}{\nu} \sum_n a_n \sum_m \left(\int_{t_i}^t dt' \exp \left[\frac{-i(t - t') E_m^{(0)}}{\nu} \right] \langle m^{(0)} | \hat{\Phi}(t') | n^{(0)} \rangle \right. \\ \left. \times \exp \left[\frac{-i(t' - t_i) E_n^{(0)}}{\nu} \right] \right) |m^{(0)}\rangle, \quad (\text{A.70})$$

where the matrix elements $\langle m^{(0)} | \hat{\Phi}(t') | n^{(0)} \rangle$ are given by

$$\langle m^{(0)} | \hat{\Phi}(t') | n^{(0)} \rangle = L^2 \int_0^L \overline{\phi_m^{(0)}(x)} \Phi(x, t') \phi_n^{(0)}(x) dx. \quad (\text{A.71})$$

Substituting Φ from (A.3) leads to

$$\langle m^{(0)} | \hat{\Phi}(t') | n^{(0)} \rangle = -\frac{\delta_a}{2} \left(\frac{d}{2\pi\tau} \right)^2 \exp \left(\frac{t - t_i}{\tau} \right) \sum_{s=\pm 1} \delta_{m,n+sN}, \quad (\text{A.72})$$

where we have made use of fact that $L = Nd$. Inserting the matrix elements (A.72) into (A.70) and evaluating the resulting integral we find that

$$|\psi^{(1)}(t)\rangle = \frac{i\delta_a}{8\pi^2\gamma} \exp \left(\frac{t - t_i}{\tau} \right) \sum_n a_n \exp \left[\frac{-i(t - t_i) E_n^{(0)}}{\nu} \right] \\ \times \sum_{s=\pm 1} \frac{1}{\zeta_{n,s}} \left(1 - \exp \left[\frac{-(t - t_i)\zeta_{n,s}}{\tau} \right] \right) |n + sN^{(0)}\rangle, \quad (\text{A.73})$$

where $\gamma = \nu\tau/d^2$ is the dimensionless parameter introduced previously and

$$\zeta_{n,s} \equiv 1 + 2is\pi\gamma(k_nd + s\pi). \quad (\text{A.74})$$

The next step is to determine the state ket $|\psi^{(2)}(t)\rangle$. The procedure is the same as that used above to calculate $|\psi^{(1)}(t)\rangle$. After a lengthy calculation we find that:

$$\begin{aligned}
|\psi^{(2)}(t)\rangle = & - \left(\frac{\delta_a}{8\pi^2\gamma} \right)^2 \exp \left[\frac{2(t-t_i)}{\tau} \right] \sum_n a_n \exp \left[\frac{-i(t-t_i)E_n^{(0)}}{\nu} \right] \\
& \times \sum_{r=\pm 1} \sum_{s=\pm 1} \frac{1}{(\zeta_{n,s} + \eta_{n,r,s})} \exp \left[\frac{-(t-t_i)\zeta_{n,s}}{\tau} \right] \\
& \times \left\{ \frac{1}{\zeta_{n,s}} \left(\exp \left[\frac{(t-t_i)\zeta_{n,s}}{\tau} \right] - 1 \right) \right. \\
& \left. + \frac{1}{\eta_{n,r,s}} \left(\exp \left[\frac{-(t-t_i)\eta_{n,r,s}}{\tau} \right] - 1 \right) \right\} |n + (r+s)N^{(0)}\rangle, \tag{A.75}
\end{aligned}$$

where $\zeta_{n,s}$ is defined as in (A.74) and

$$\eta_{n,r,s} \equiv 1 + 2ir\pi\gamma[k_n d + (r+2s)\pi]. \tag{A.76}$$

Appendix A.3.2. Summary We have used time-dependent perturbation theory to find a second-order approximate solution $|\psi(t)\rangle$ of the Schrödinger equation (A.4) with a time-dependent sinusoidal potential. The solution is of the form

$$|\psi(t)\rangle = \sum_{j=0}^2 |\psi^{(j)}(t)\rangle, \tag{A.77}$$

where $|\psi^{(0)}(t)\rangle$, $|\psi^{(1)}(t)\rangle$ and $|\psi^{(2)}(t)\rangle$ are given by (A.69), (A.73) and (A.75) respectively. In the position representation (A.76) becomes

$$\psi = \sum_{j=0}^2 \psi^{(j)}, \tag{A.78}$$

with $\psi^{(j)} = \psi^{(j)}(x, t)$ defined by $\psi^{(j)} = \langle x | \psi^{(j)}(t) \rangle$. The zeroth-order wavefunction $\psi^{(0)}$ is then given by

$$\psi^{(0)} = \sum_n a_n \exp \left[\frac{-i(t-t_i)E_n^{(0)}}{\nu} \right] \phi_n^{(0)}, \tag{A.79}$$

where the eigenfunctions $\phi_n^{(0)} = \phi_n^{(0)}(x)$ are given by (A.14), $E_n^{(0)} = \nu^2 k_n^2 / 2$, $k_n = 2n\pi/L$ and $L = Nd$. The expansion coefficients are found from (A.21) and are zero unless n is an integer multiple of N . In a similar fashion it is straightforward to show that

$$\begin{aligned}
\psi^{(1)} = & \frac{i\delta_a}{8\pi^2\gamma} \exp \left(\frac{t-t_i}{\tau} \right) \sum_n a_n \exp \left[\frac{-i(t-t_i)E_n^{(0)}}{\nu} \right] \phi_n^{(0)} \\
& \times \sum_{s=\pm 1} \frac{1}{\zeta_{n,s}} \left(1 - \exp \left[\frac{-(t-t_i)\zeta_{n,s}}{\tau} \right] \right) \exp \left(\frac{2is\pi x}{d} \right), \tag{A.80}
\end{aligned}$$

and

$$\begin{aligned}
\psi^{(2)} = & - \left(\frac{\delta_a}{8\pi^2\gamma} \right)^2 \exp \left[\frac{2(t - t_i)}{\tau} \right] \sum_n a_n \exp \left[\frac{-i(t - t_i)E_n^{(0)}}{\nu} \right] \phi_n^{(0)} \\
& \times \sum_{r=\pm 1} \sum_{s=\pm 1} \frac{1}{(\zeta_{n,s} + \eta_{n,r,s})} \exp \left[\frac{-(t - t_i)\zeta_{n,s}}{\tau} \right] \\
& \times \left\{ \frac{1}{\zeta_{n,s}} \left(\exp \left[\frac{(t - t_i)\zeta_{n,s}}{\tau} \right] - 1 \right) \right. \\
& \left. + \frac{1}{\eta_{n,r,s}} \left(\exp \left[\frac{-(t - t_i)\eta_{n,r,s}}{\tau} \right] - 1 \right) \right\} \exp \left[\frac{2i(r+s)\pi x}{d} \right], \tag{A.81}
\end{aligned}$$

where $\zeta_{n,s}$ and $\eta_{n,r,s}$ are given by (A.74) and (A.76) respectively.

References

Bagla J S and Padmanabhan T 1994 *Mon. Not. R. Astron. Soc.* **266** 227
 Bardeen J M 1980 *Phys. Rev. D* **22** 1882
 Bernardeau F, Colombi S, Gaztanaga E and Scoccimarro R 2002 *Phys. Rep.* **367** 1
 Bloch F 1928 *Zts. f. Phys.* **52** 555
 Brainerd T G, Scherrer R J and Villumsen J V 1993 *Astrophys. J.* **418** 570
 Bruni M, Dunsby P K S and Ellis G F R 1992 *Astrophys. J.* **395** 34
 Cichowlas C, Bonaiti P, Debbasch F and Brachet M 2005 *Phys. Rev. Lett.* **95** 264502
 Coles P 2002 *Mon. Not. R. Astron. Soc.* **330** 421
 Coles P, Melott A L and Shandarin S F 1993 *Mon. Not. R. Astron. Soc.* **260** 765
 Coles P and Spencer K 2003 *Mon. Not. R. Astron. Soc.* **342** 176
 Gurbatov S N, Saichev A I and Shandarin S F 1989 *Mon. Not. R. Astron. Soc.* **236** 385
 Hawking S W 1966 *Astrophys. J.* **145** 544
 Husimi K 1940 *Proc. Phys. Math. Soc. Japan* **22** 264
 Kodama H and Sasaki M 1984 *Prog. Theor. Phys. Suppl.* **78** 1
 Kodama H and Sasaki M 1987 *Int. J. Mod. Phys. A* **2** 491
 Lifshitz E M 1946 *Sov. Phys. JETP* **10** 116
 Madelung E 1926 *Zts. f. Phys.* **40** 322
 Mukhanov V F, Feldman H A and Brandenberger R H 1992 *Phys. Rep.* **215** 203
 Peebles P J E 1980 *The Large-scale Structure of the Universe* (Princeton University Press)
 Sahni V and Coles P 1995 *Phys. Rep.* **262** 1
 Short C J and Coles 2006 *to be submitted*
 Skodje R T, Rohrs H W and VanBuskirk J 1989 *Phys. Rev. A* **40** 2894
 Szapudi I and Kaiser N 2003 *Astrophys. J.* **583** L1
 Widrow L M and Kaiser N 1993 *Astrophys. J.* **416** L71
 Widrow L M 1997 *Phys. Rev. D* **55** 10
 Zeldovich Ya B 1970 *Astron. Astrophys.* **5** 84